X-733-69-554

NASA TM X- 63834

EXPERIMENTAL REPORT ON 16 GHZ AND 35 GHZ RADIOMETERS ASSOCIATED WITH THE ATS-V MILLIMETER WAVE EXPERIMENT

YUICHI OTSU

NOVEMBER 1969

GSFC

GODDARD SPACE FLIGHT CENTER
GREENBELT, MARYLAND

X-733-69-554

EXPERIMENTAL REPORT ON 16 GHZ AND 35 GHZ RADIOMETERS ASSOCIATED WITH THE ATS-V MILLIMETER WAVE EXPERIMENT

Yuichi Otsu

November 1969

Goddard Space Flight Center
Greenbelt, Maryland

PRECEDING PAGE BLANK NOT FILMED

CONTENTS

CONTENTS–(continued)

EXPERIMENTAL REPORT ON 16 GHZ AND 35 GHZ RADIOMETERS ASSOCIATED WITH THE ATS-V MILLIMETER WAVE EXPERIMENT

Yuichi Otsu

ABSTRACT

An experiment on the 16 GHz and 35 GHz radiometers that are to be used in connection with the ATS-V Millimeter Wave Experiment was carried out during June and July 1969 at Goddard Space Flight Center to measure sky temperature, and to estimate the antenna loss factor and the long time drift, which cause antenna temperature increase and error in temperature measurements, respectively.

The relation between the rainfall rate at one point and the temperature increase due to rain and rain cloud is described.

Some aspects about the temperature scintillation due to cloud are also discussed. Sky temperature calculations have been made for a standard atmospheric model and other precipitation conditions.

PRECEDING PAGE BLANK NOT FILMED.

EXPERIMENTAL REPORT ON 16 GHZ AND 35 GHZ RADIOMETERS ASSOCIATED WITH THE ATS-V MILLIMETER WAVE EXPERIMENT

Yuichi Otsu

FOREWORD

Mr. Yuichi Otsu is a member of the staff of the Radio Research Laboratories, Ministry of Posts and Telecommunications, Tokyo, Japan. Since November 1968, Mr. Otsu has been performing studies and experiments at Goddard Space Flight Center, Greenbelt, Maryland, in relation to the Millimeter Wave Propagation Experiment being flown on NASA's fifth application technology satellite (ATS-V).

During the past decade, NASA and the Ministry of Posts and Telecommunications have had continuing cooperative endeavors with respect to earth/space communications, particularly as associated with the ATS Program. Inasmuch as the communication bands at microwave frequencies are overcrowded, attention is being focused on the possible use of millimeter wave frequencies to meet the increasing communication demands of the future. Unfortunately, millimeter wave frequencies suffer losses from atmospheric water vapor conditions – the weather. Numerous propagation studies have been made of terrestrial millimeter wave characteristics as affected by prevailing and ever-changing meteorological conditions. Since surface conditions differ from that of the upper atmosphere, if earth/space millimeter wave communication systems are to be realized, it is necessary to measure the losses along the propagation path from ground to satellite. Hence, engineers at Goddard Space Flight Center designed an experiment for implementation in connection with the ATS-V. For this purpose 15.3 GHz and 31.65 GHz signal characteristics as transmitted to the earth and to the satellite respectively are to be measured and related to meteorological conditions. Since weather patterns change and vary throughout the world it becomes necessary to make earth/space measurements from as many localities as possible; hence the experiment was designed to permit a cooperative endeavor. Scientists at the Ministry of Post and Telecommunications, among others, signified their desire to participate. However, since the ATS-V was designed for geostationary orbit and it was decided to "park" it at 108° West longitude, foreign participation was to be excluded. As a result, an exchange program between NASA and the Ministry of Post and Telecommunications was consummated, which provided for a staff member of the Radio Research Laboratories to work at Goddard Space Flight Center and assist with the implementation of the experiment. Mr. Otsu was selected to serve this tenure, his previous work in terrestial millimeter wave link studies uniquely qualifying him for this duty.

As was previously mentioned, the measured millimeter wave signal characteristics must be related to the prevailing measured meteorological conditions existing between the ground terminal and the satellite. This raises the question of what surface-based instrumentation can be used to measure the conditions upward through the atmosphere. The radiometer, which provides a measure of sky temperature dependent on water vapor content, is one such instrument deemed worthy of deployment during the experiment. Therefore GSFC personnel built two radiometers for this purpose. Upon Mr. Otsu's joining the experiment staff he was asked to test and evaluate these instruments prior to their deployment at a ground terminal. This document was prepared by Mr. Otsu to record the experiments and analysis which he performed on the radiometers. He is to be commended for his effort, both from the standpoint of making a significant technical contribution to the ATS-V Millimeter Wave Experiment and for his rapid attainment of an ability to use the English language during his tenure. This report reflects these accomplishments.

In conclusion it should be noted that the first ATS-V Millimeter Wave signals were received by Ground Terminal stationed at Rosman, North Carolina on September 27, 1969, and that Mr. Otsu assisted with the installation of the radiometers at the site.

EXPERIMENTAL REPORT ON 16 GHZ AND 35 GHZ RADIOMETERS ASSOCIATED WITH THE ATS-V MILLIMETER WAVE EXPERIMENT

1. INTRODUCTION

A new and higher-frequency microwave region (over 10 GHz) is necessary for future space-to-ground and space-to-space communication. At these microwave frequencies, there exist many disturbances in the atmosphere. For example, atmospheric gaseous attenuation and precipitation losses are much greater for frequencies over 30 GHz than for frequencies around 10 GHz. Therefore, it is a fundamental necessity to investigate the character of propagation through atmosphere of the microwave frequencies. One of the equipments used for such investigations is the radiometer. It shows the noise temperature of the sky at a certain frequency, which corresponds exactly to the attenuation through the atmosphere. Thus the radiometer is very useful for investigating millimeter wave space communication links. The purpose of this experiment was to check the antenna loss and feeder loss of the 16 GHz and 35 GHz radiometers that will provide comparative data for the ATS-V Millimeter Wave Experiment and to provide some information on the temperature increase due to rain and cloud. Calculations of sky temperature for clear, cloudy, and rainy days have been carried out using some standard models of the atmosphere. The daily changes of the atmosphere have a statistical feature; therefore, in connection with the communication studies, a statistical treatment of the data must be employed.

2. SYSTEMS DESCRIPTION

The two radiometers that will be used in the NASA ATS-V Millimeter Wave Experiment at the Rosman, North Carolina station were put in operation at Goddard Space Flight Center (GSFC), Greenbelt, Maryland for preliminary measurements of sky temperature, calibration, and checks of system stability. The diagrams and the characteristics of the two radiometers are shown in Figure 2.1 and Table 2.1. These radiometers are of normal "Dicke" type and the principal difference between both radiometers is the mechanical modulator at 16 GHz and the ferrite modulator at 35 GHz, as shown in Figure 2.1.

For this experiment, being conducted at GSFC, the radiometers were located in a parking lot adjacent to Building 22 as shown in Figure 2.2. The building is 45 feet high. The locations of other buildings and surrounding trees are also shown in Figure 2.2. The azimuth and elevation angles of the radiometers

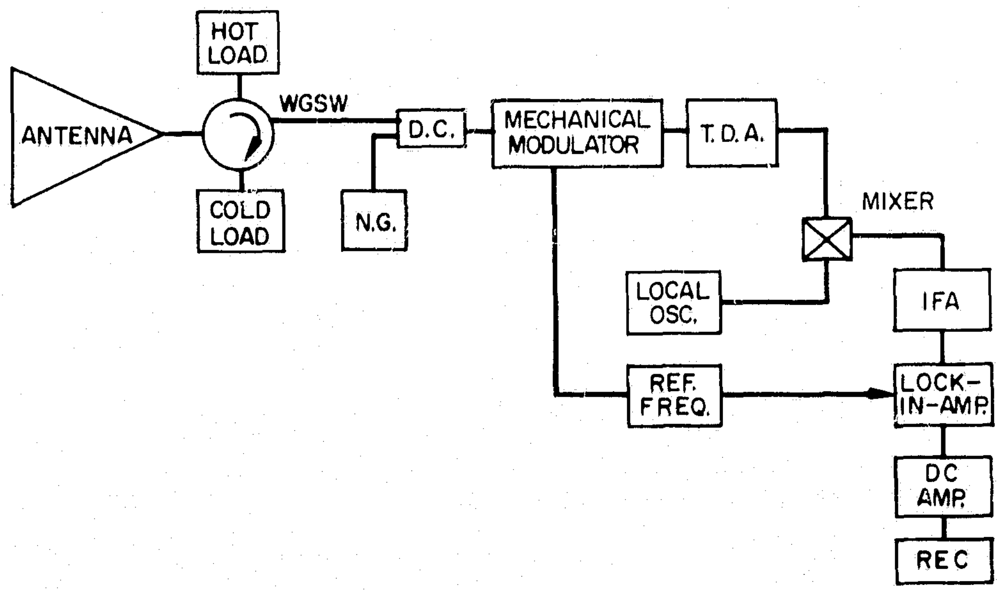

Figure 2.1(a). Block diagram for 16 GHz radiometer.

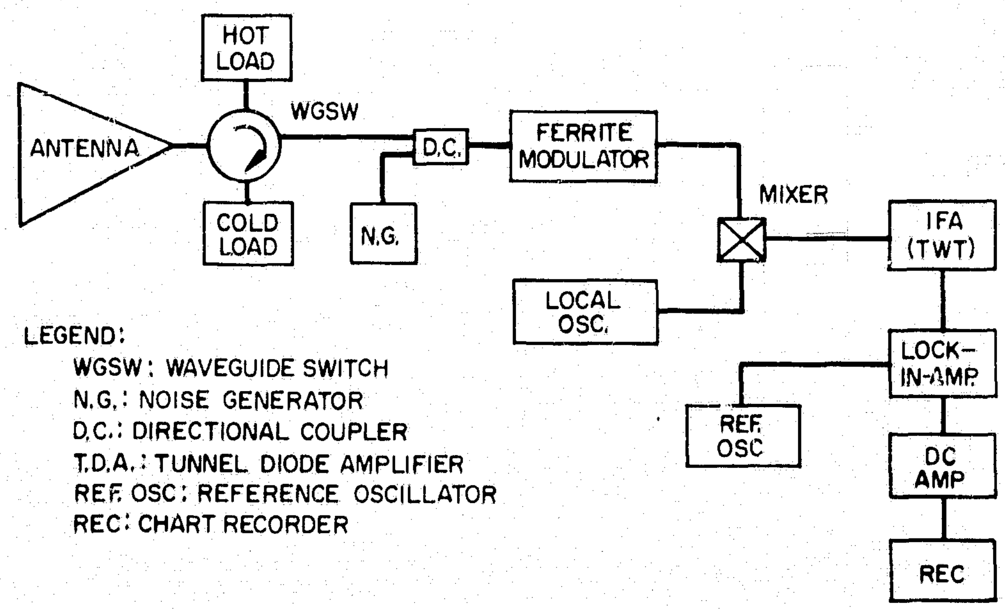

Figure 2.1(b). Block diagram for 35 GHz radiometer.

Table 2.1
Characteristics of the two Radiometers

Characteristic	16 GHz Radiometer	35 GHz Radiometer
Antenna	TRG Lens Ant.	TRG Lens Ant.
Diameter	12 inch	12 inch
Gain	32 dB	39 dB
Matching (VSWR)	< 1.01	<1.01
Antenna efficiency	~0.8	~0.8
Beam width	4.0°	2.0°
RF Amp.	T.D.A. 15 dB (NF7dB)	Not used.
IF Amp.		
Bandwidth	80 MHz	2.0 GHz
Noise Figure	6 dB	12 dB
Local Oscillators	Klystron (Varian)	Klystron (Varian)
Modulator	Mechanical	Ferrite Switching
Mod. Freq.	94 100 Hz	94 100 Hz
Recorder		
Amp.	Lock-in Amp	Lock-in Amp
Out	0 - 5V	0 - 5V
Sensitivity $\left(= K \frac{T_{sys}}{\sqrt{Bt}}\right)$ (t=1 sec k= 2	0.22°K	0.45°K
Ambient temp. of radiometer (RF, IF)	40°C ± 1°C	40°C ± 1°C
Hot load	318°K (45°C)	318°K (45°C)
Cold load	Liquid Nitrogen (77°K), dry ice (198°K) or ice cubes (273°K)	

Figure 2.2(a). Radiometer location.

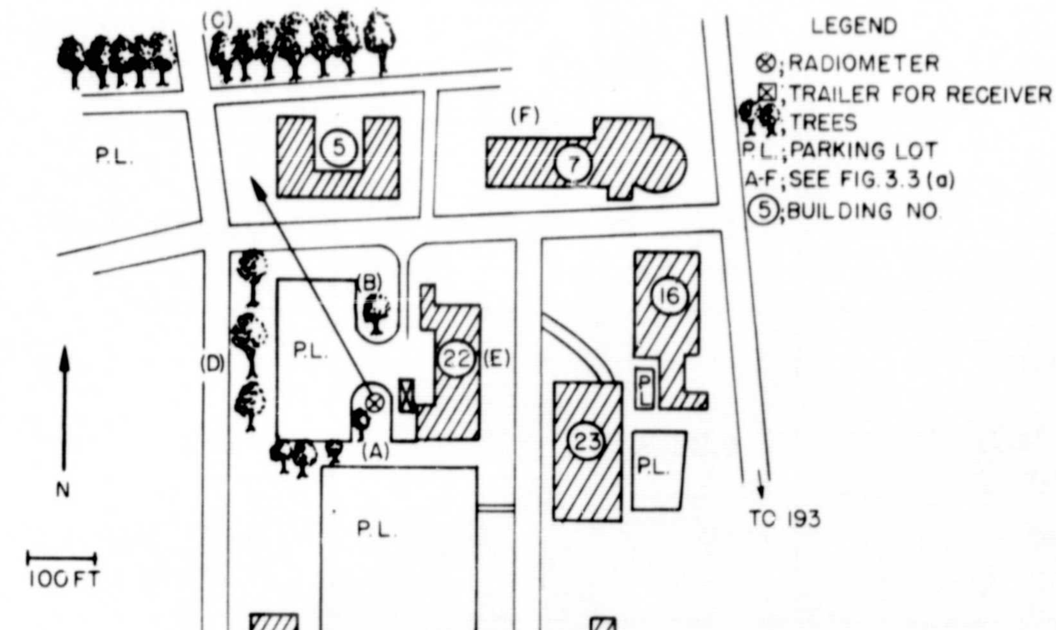

Figure 2.2(b). Enlarged view of experimental site at GSFC.

could be adjusted. Temperature, humidity, and rainfall rate (a single bucket-type gauge) measurements were made using instruments located near the radiometers. These measurements were always checked against Weather Bureau data in Washington.

3. SKY TEMPERATURE ESTIMATION

3.1 Temperature Estimation Method.

To carry out accurate measurements of sky temperature, the waveguide losses must be known since they appear as a certain temperature increase at the recorder. The waveguide losses for hot and cold load were measured by the power meter method at 16 and 35 GHz. The data are given in Table 3.1 and 3.2.

Table 3.1
16 GHz Feeder Losses and α

Type of Loss	Loss (dB)	Fractional transmission Coefficient (α)	$1/\alpha$
Antenna	0.9 dB	0.813	1.23
Hot load loss	0.95 dB	0.804	1.24
Cold load loss	1.15 dB	0.767	1.30

(The antenna loss 0.9 dB was calculated by assuming the antenna efficiency of $\eta = 0.8$. Therefore, the exact antenna and feeder losses must be determined by other methods.)

Table 3.2
35 GHz Feeder Losses and α

Type of Loss	Loss (dB)	Fractional Transmission Coefficient (α)	$1/\alpha$
Antenna	1.30	0.741	1.35
Hot load loss	1.40	0.725	1.38
Cold load loss	1.40	0.725	1.38

3.1.1 Sky temperature expectation at 16 GHz.

By using the values in Table 3.1, the measured sky temperature can be derived from

$$T_d = T_s \cdot \alpha + T_{amb} \cdot (1 - \alpha) \tag{3.1}$$

where

T_d Dicke Temperature (the temperature at the input to Dicke switch which can be converted to a nominal value on the recorder);

T_s Sky Temperature;

T_{amb} Ambient temperature inside the box, which causes the temperature increase effect upon Dicke Temperature.

For hot load,

$$T_s = T_H = 273 + 45^\circ\ C = 318^\circ\ K,$$

$$T_{amb} = 273 + 40^\circ\ C = 313^\circ\ K,$$

$$\alpha = 0.804;$$

therefore

$$T_d = 317.0^\circ\ K.$$

For cold load

$$T_s = T_c = 77^\circ\ K,$$

$$T_{amb} = 313^\circ\ K,$$

$$\alpha = 0.767;$$

therefore

$$T_d = 132^\circ\ K.$$

For the antenna: Under the assumption that the scale of the recorder is linear (see appendix 1.1), we can calculate T_s from Equation (3.1) as follows:

$$T_d = T_s \cdot \alpha + T_{amb}\,(1 - \alpha),$$

$$T_s = \frac{1}{\alpha} T_d - \frac{T_{amb}}{\alpha}(1 - \alpha)$$

Since

$$\alpha = 0.813 \text{ and } T_{amb} = 313° \text{ K},$$

$$T_s = 1.23\, T_d - 72. \tag{3.2}$$

For a quick determination, Figure 3.1 is convenient. The sky temperature T_s can be read directly from Figure 3.1 for various recorded Dicke temperatures T_d. Equation (3.2) must be revised later, because of the assumed antenna loss.

3.1.2 Sky temperature expectation at 35 GHz.

By using equation (3.1), Dicke temperature T_d for the hot load, cold load and antenna are calculated as follows:

For a hot load:

$$\alpha = 0.725,\ T_{amb} = 313° \text{ K},\ T_H = 318° \text{ K};$$

thus

$$T_d = 317° \text{ K}.$$

For a cold load:

$$\alpha = 0.725,\ T_{amb} = 313° \text{ K},\ T_c = 77° \text{ K};$$

thus

$$T_d = 142° \text{ K}.$$

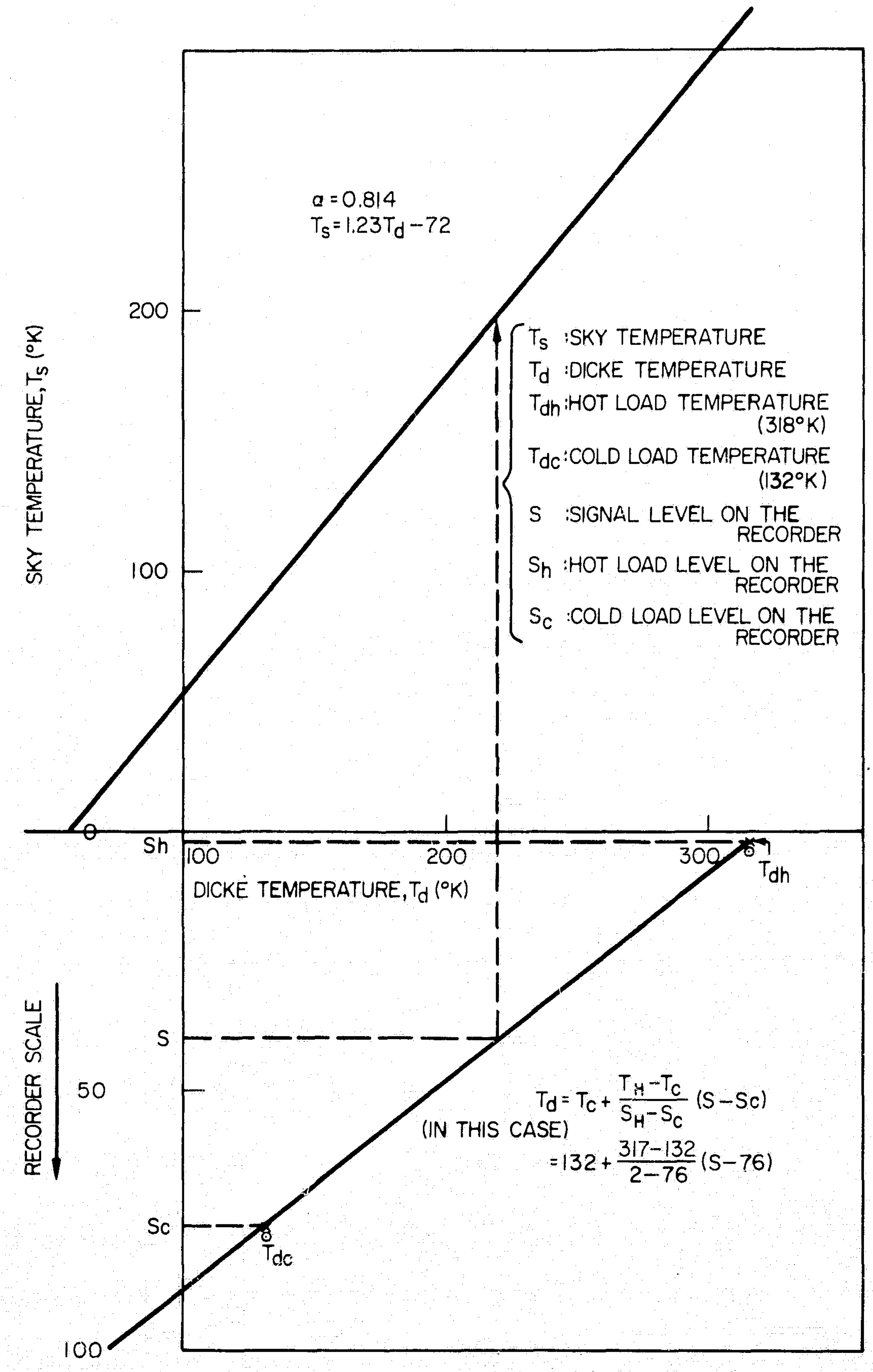

Figure 3.1. Temperature reading for the 16 GHZ radiometer.

For the antenna:

$$T_A = 1.35\, T_d - 110. \qquad (3.3)$$

The sky temperature can be determined from Figure 3.2; which is also subject to change as mentioned in 3.1.1.

3.2 Comparison between the Measured Sky Temperature and the Expected True Sky Temperature.

After calibration with hot and cold loads, the sky temperature can be obtained by using equations (3.2) and (3.3) in section 3.1.

In this case, antenna losses have been assumed to be 0.9 dB for 16 GHz, and 1.3 dB for 35 GHz. Thus the exact losses must be measured for the true sky temperature. Many ways of obtaining the value of antenna losses can be found, but the easiest way is to compare the expected true value and the measured one (including some assumptions), in order to know the difference between them. The differences between them can be regarded as due partly to antenna and waveguide losses, and partly to the antenna pattern. The differences between the measured and the expected true sky temperature are shown in Tables 3.3 and 3.4. In addition, these tables contain measured data and time, the absolute humidity, the expected true and measured sky temperatures, and the sky temperatures calculated using the equations derived by some other authors (Reference 1 and 2). The humidity is that obtained from the Weather Bureau near the time and the place measured. The expected true sky temperature was calculated (Reference 3 and 4) by converting the vertical loss into the true sky temperature at the 45° elevation angle.

The 16 GHz radiometer indicated large differences in temperature before and after calibration. This could have been due to an observed intermittent function of the waveguide switch. The averages of the differences between the measured and the expected true sky temperature are 35°K at 16 GHz and 24°K at 35 GHz. Equations (3.2) and (3.3) must be changed, to take these differences into account. The true sky temperatures at 16 GHz and 35 GHz, using the same values of Dicke temperature T_d as in equations (3.2) and (3.3), are

$$\text{For } 16\text{ GHz} \quad T_s = 1.39\, T_d - 121; \qquad (3.2A)$$

and

$$\text{for } 35\text{ GHz} \quad T_s = 1.50\, T_d - 157. \qquad (3.3A)$$

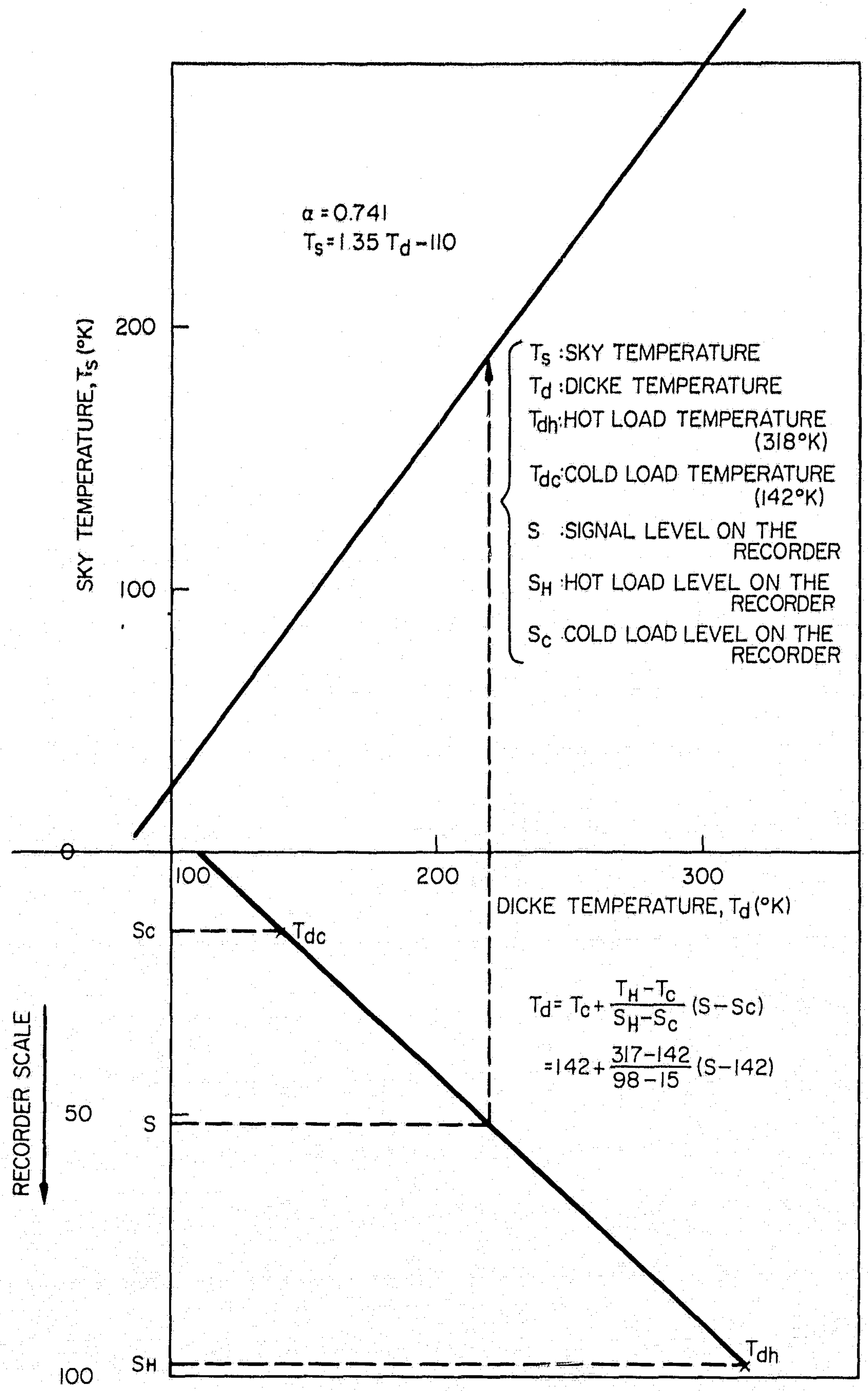

Figure 3.2. Temperature reading for the 35 GHz radiometer.

Table 3.3
Comparison Between the Measured and the Expected True Sky Temperature

For 16 GHz at 45° Elevation Angle
(Sky not cloudy)

Date	Time	Absolute Humidity (g/m^3)	Expected True Sky Temperature (°K)	$\alpha = 0.813$ Measured Temperature (°K)	Temperature Difference (°K)	Reference (expected)	
						Shulkin Reference 1 (°K)	Bean and Dutton, Reference 2 (°K)
6/25	16.50	15	11	B 37	26	(8)	(8)
			11	A 46	35		
6/26	16.30	16	11	45	34	(8)	(8.5)
6/28	16.30	19	12	51	39	10	9.5
6/29	18.30	10	9	53	44	(6.4)	(6.5)
6/30	17.05	11	9	B 54	45	(7)	(7)
			9	A 70	61*		
7/1	17.40	13	10	B 64	54*	8	7.5
			10	A 46	36		
7/2	16.20	11.5	9	B 34	15	7	7
			9	A 39	30		

Average temperature difference: 35°K

*; waveguide switch malfunction
B; Before calibration
A; After calibration
(); interpolated

Table 3.4

Comparison Between the Measured and the Expected True Sky Temperature

For 35 GHz at 45° Elevation Angle
(sky not cloudy, except as noted)

Date	Time	Absolute Humidity (g/m^3)	Expected True Sky Temperature (°K)	$r = 0.741$ Measured Temperature (°K)	Temperature Difference (°K)	Reference (expected)	
						Shulkin Reference 1 (°K)	Bean and Dutton, Reference 2 (°K)
6/25	16.50	15	32	64	32	27	32
6/26	16.30	16	33	60	27	(28.5)	(33)
6/27	17.30	18	35	60	25	31	36
6/28	16.30	19	35	71	36*	(31.5)	(37)
6/29	18.30	10	26	51	25	(20.5)	(26)
6/30	17.05	11	27	B 50	23	(22)	(27)
				A 77	50*		
7/1	17.40	13	30	48	18	(24)	(30)
7/2	16.20	11.5	28	40	12	23	28
7/3	16.00	12	29	B 68 (CL)	39*	(24)	(28)
				A 50	21		

Average temperature difference: 24°K
*; Waveguide switch malfunction
B; Before calibration
A; After calibration
(); Interpolated
CL; Partly cloudy

As already mentioned, these differences are due to antenna patterns and antenna losses, including those of the waveguide switch. The antenna pattern effects will be considered in the next section.

3.3 Surrounding Circumstance Effects on the Radiometer Temperature

In this section we describe an approximate method for determining the value of the sky temperature increase due to the trees and buildings.

Both radiometers were located near Building 22 at GSFC, which was not an ideal place (Fig. 3.3a). Therefore, some temperature increase due to the sidelobes must be expected during measurement of sky temperature.

3.3.1 Approximation of the energy distribution angle for both radiometer antennas

First, the antenna energy distribution patterns must be known for the estimation of the temperature increase due to sidelobes around 360°. However, for this experiment, the antenna patterns were not available*, and for that reason an approximate energy distribution was derived from Reference 5, and was

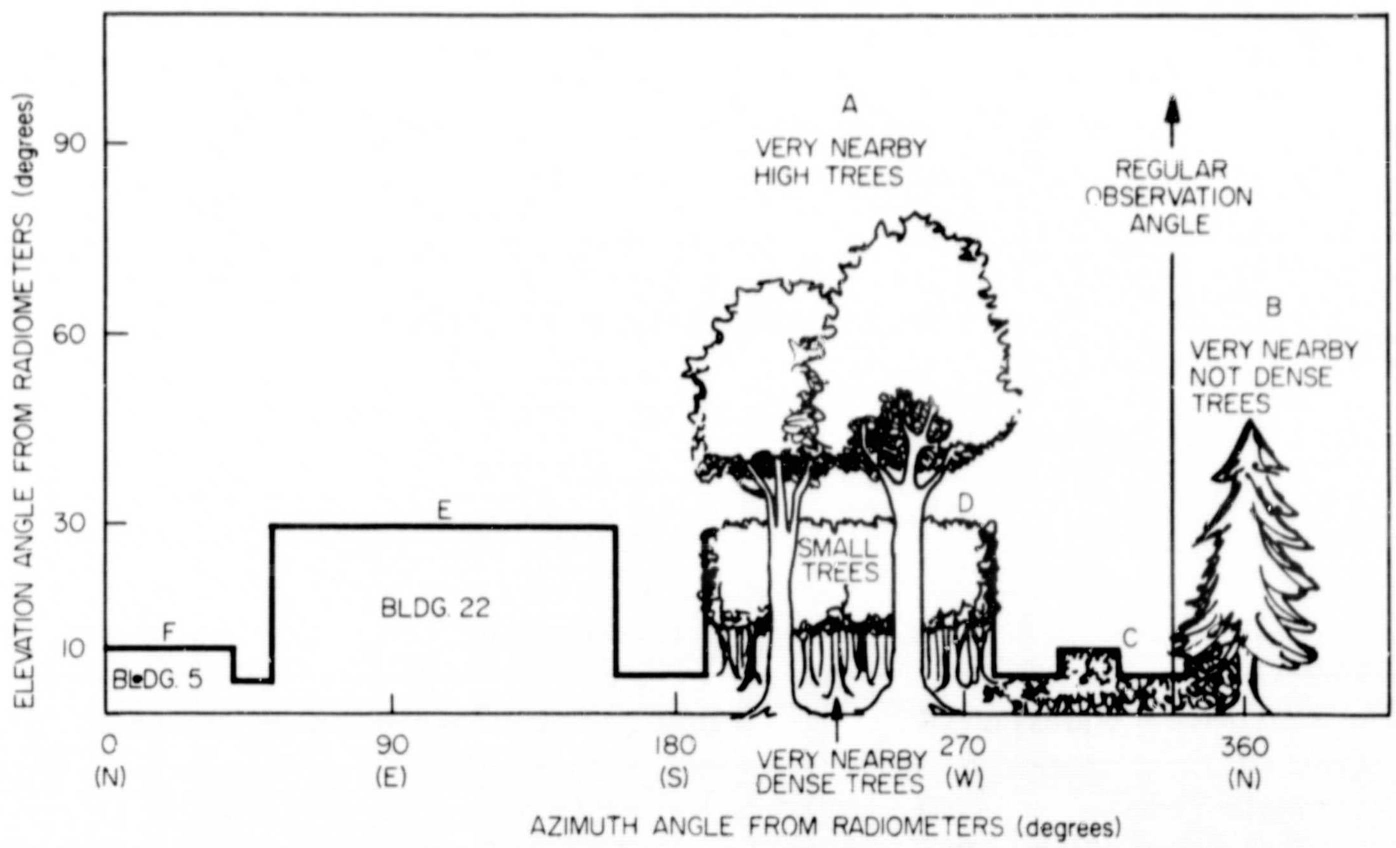

Figure 3.3(a). Surrounding features.

*See Appendix 4 correction.

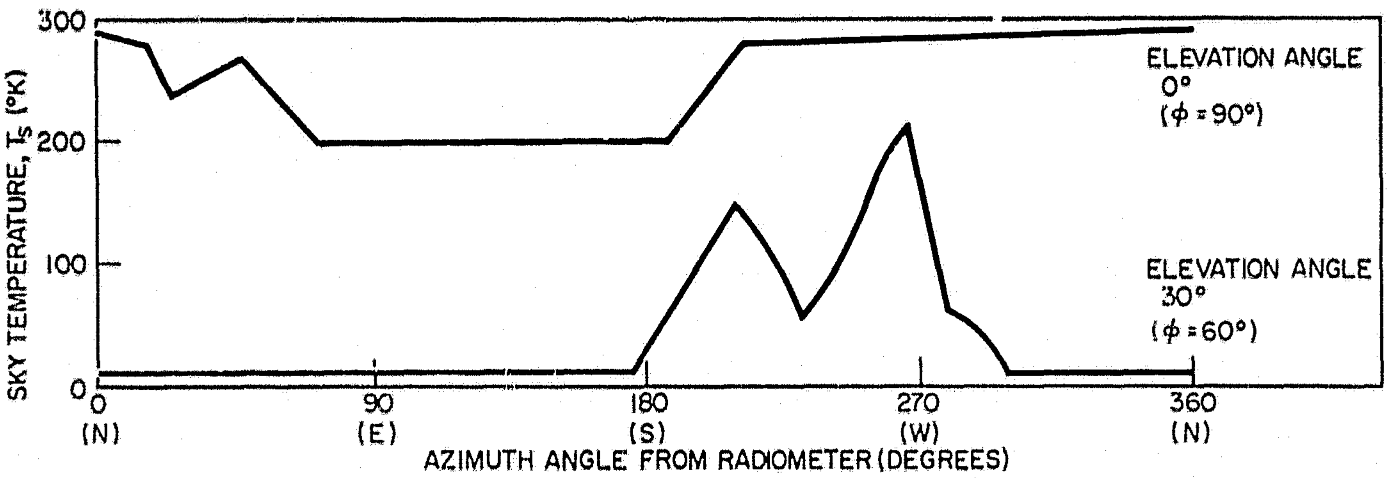

Figure 3.3(b). Surrounding temperature at 15 GHz.

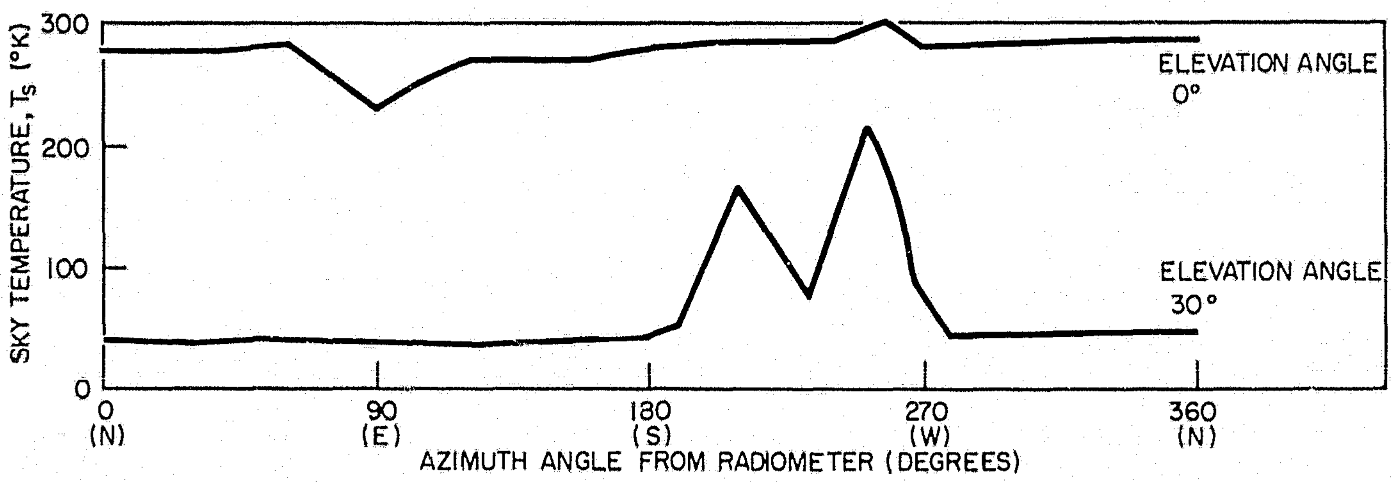

Figure 3.3(c). Surrounding temperature at 35 GHz.

Table 3.5
Antenna Energy Distribution

Value from Reference 5		Modified value for the 1-foot Antenna	
Main Lobe	70%	Main lobe (~ 2°)	70%
Side lobes (0-3°)	23%	Side lobes (2~12°)	23%
Side lobes (3-7°)	5%	Side lobes (12~30°)	5%
Side lobes (7-180°)	2%	Side lobes (30~180°)	2%

modified according to the size of our antennas. In Table 3.5 are shown the values from Reference 5 and the modified distribution angle for the 1-foot antenna of the 35 GHz radiometers. The values of the distribution angle from Reference 5 are applicable for most "large" antennas, for which diameters can be supposed to be larger than 1 meter. Therefore, in this case, the 35 GHz antenna (diameter 1 foot) is about 4 times smaller than most "large" antennas, and the distribution angles in Table 3.5 become 4 times larger than those for the large antennas. For the 16 GHz antenna, the distribution angles become twice as great as those of the 35 GHz antenna. As indicated in Table 3.5, 98% of all the incoming energy of the antennas is included within 30° at 35 GHz and 60° at 16 GHz.

3.3.2 Sky temperature increase due to the side lobes for 35 GHz radiometers (at zenith)

The modified energy distribution is only approximate for our antenna. Therefore when the sky temperature increase due to sidelobes hitting trees and buildings is calculated, the following experimental procedures are necessary for estimating the sky temperature increase at zenith.

1. The measured and calculated dependence of sky temperature along the zenith angle, ϕ, in the direction of daily observation is plotted in Figure 3.4.

2. In the top of Figure 3.4 is shown the temperature difference due to the deviation from the secant ϕ law, which probably is caused by the sidelobes (see Figure 3.5 (b) A) hitting the trees, C, in Figure 3.3.(a).

3. When the antenna is tipped from zenith to horizen, other sidelobes (see Figure 3.5.(a)) besides those which hit the trees C have constant effects upon the sky temperature increase; these will be calculated in following paragraphs.

4. The sky temperature increases due to trees and buildings, excepting trees A and B (see Figure 3.3(a)), are considered first. The deviation value of sky temperature at 30° zenith angle (top of Figure 3.4 and also Figure 3.6(a)) can be applied to the case when the antenna main beam has a 60° difference in angle from the trees D, which surrounded the radiometer at the 30° elevation angle (Figure 3.3 (a) and 3.6 (b)). Therefore, the following formula can be introduced for calculating the temperature increase due to sidelobes:

$$\Delta t = \frac{\Delta T \times \beta}{\alpha} = 3° \text{ K}, \qquad (3.4)$$

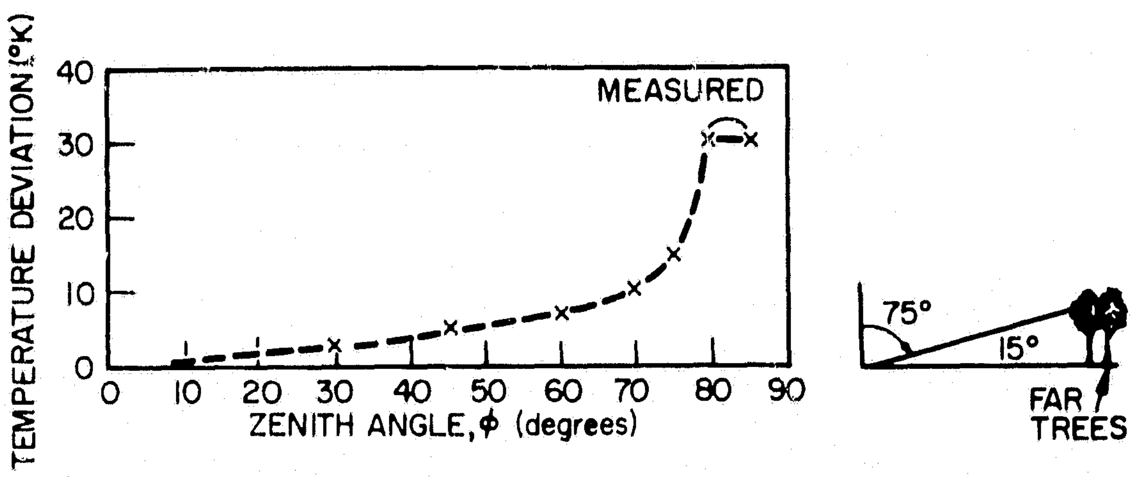

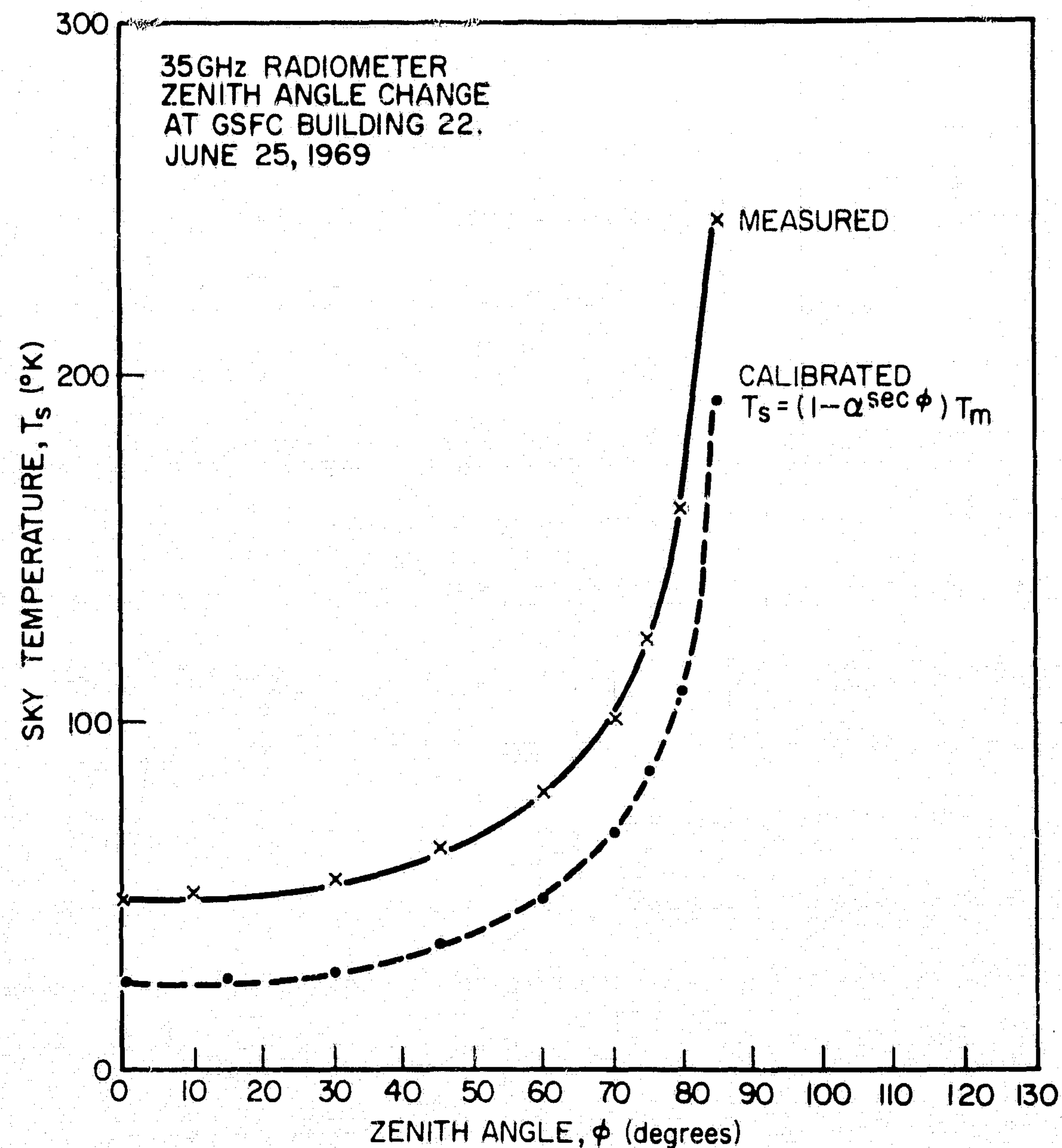

Figure 3.4 Secant ϕ pattern.

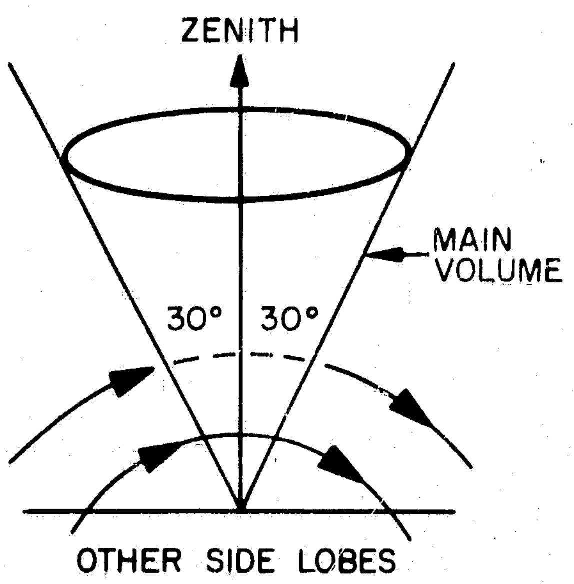

Figure 3.5(b). Scanning along the ϕ direction.

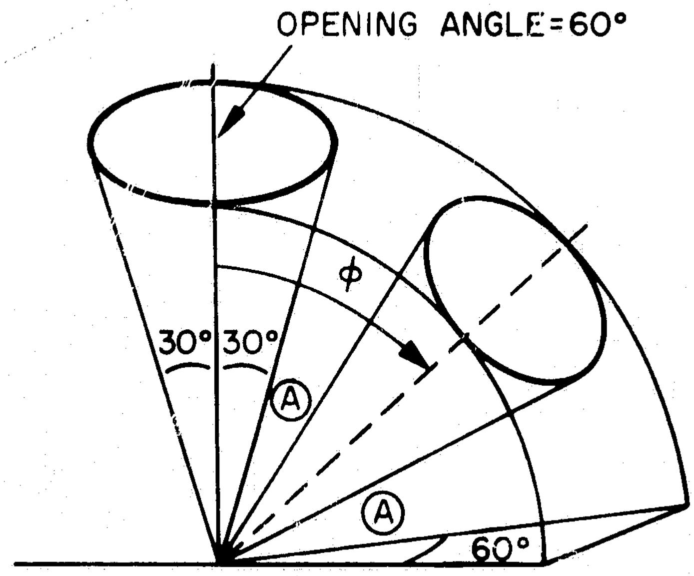

Figure 3.5(a). Main volume and other side lobes along the side of the volume.

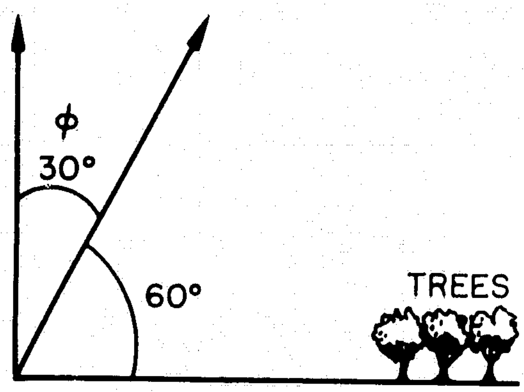

Figure 3.6(a). Angle difference between the main beam and trees when measured. (See ϕ pattern).

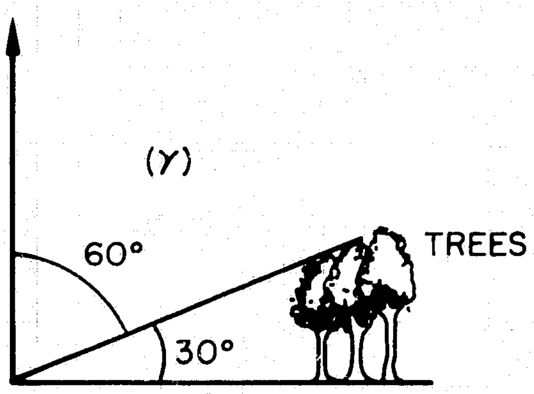

Figure 3.6(b). Angle difference between the main beam 8at zenith) and trees.

where

Δt = sky temperature increase due to sidelobes hitting trees "D" in Figure 3.3 (a),

ΔT = sky temperature increase at the $\gamma = 60°$ angle difference between the main beam and trees "D" in Figure 3.3 (a),

β = angle of horizontal spreading of the trees "D" at 30° elevation angle (90°)

α = volumes which can be supposed to have 98% of all energy in the ideal antenna of this type (60°, in this case).

As for the buildings surrounding the antenna (see Figure 3.3 (a) E, F), the temperature increase effect due to sidelobes can be neglected even if they are at a 30° elevation angle. The reason is that when the horizontal sweep is made at a 30° elevation angle, (see Figure 3.3 (c)) the sky temperatures are 3 - 7°K less in the sky temperature compared to the temperature near "C" in Figure 3.3 (a).

5. Using the equation (3.4) as in paragraph 4, the sky temperature increase due to the trees A can be obtained as follows:

$$\Delta t = \frac{\Delta T \times \beta}{\alpha} = 2.5° \text{ K},$$

where $\Delta T = 7.5°K$ is obtained from the angle difference γ between the main beam and the trees "A", ($\gamma = 20°$ in this case) corresponding to $\phi = 70$ (Figure 3.4) so the temperature increase ΔT at $\phi = 70°$, is 7.5°K); $\beta = 20°$ = the opening angle; and $\alpha = 60°$ = the main volume (see Figure 3.7(a) and (b)).

6. The temperature increase due to the trees "B" can be calculated easily just as in paragraph 4:

$$\gamma = 45°, \ \beta = 10°, \ \Delta T = 4° \text{ K},$$

$$4° \text{ K} \times \frac{10}{60} = 0.67 \sim 1° \text{ K}.$$

7. The sky temperature increase due to sidelobes which are directed towards the ground is (Figure 3.8): A 2°K temperature increase from the ground can be expected for 35 GHz radiometers.

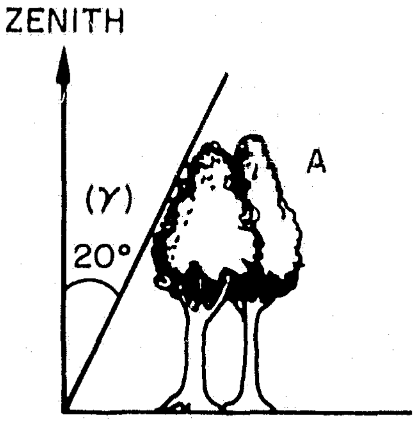

Figure 3.7(a). Angle difference between the main beam and trees "A".

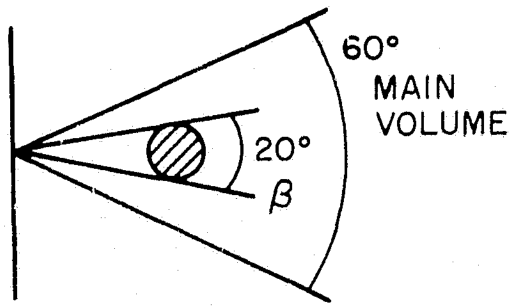

Figure 3.7(b). Horizontal spreading angle β: opening angle.

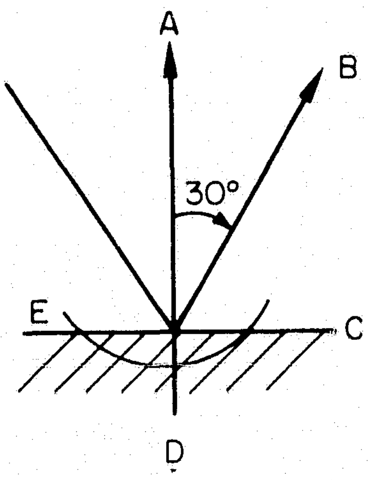

Figure 3.8. Geometry of the main volume, sidelobes, and ground

8. Overall, at zenith, temperature increase due to sidelobes is approximately 8.5°K (3 + 2.5 + 1 + 2) for the 35 GHz radiometer.

3.3.3 Sky temperature increase due to the sidelobes for the 16 GHz radiometer (at zenith)

The secant ϕ pattern was measured for the 16 GHz radiometer at the same time as the one for the 35 GHz radiometer. However, the temperature increase due to sidelobes cannot be found distinctly until the tipping angle is larger than 60° from zenith. From the measured values (not shown here), temperature increase can be estimated as follows.

For trees D at elevation angle 30° (see Figure 3.3 (a) the temperature increase is "negligible."

For tree A, which is 20° from the main beam,

$$3^\circ \text{ K} \times \frac{20}{120} = 0.5^\circ \text{ K}.$$

For trees B, the temperature increase is "negligible."

For the temperature increase due to the sidelobes looking at the ground, the calculation can be done in the same way as in (g) of 3.3.1:

$$295^\circ \text{ K} \times \frac{180}{360 - 120} \times 2\% = 4^\circ \text{ K}.$$

Thus the total temperature increase due to all the sidelobes of a 1-foot antenna at 16 GHz is

$$4^\circ \text{ K} + 0.5^\circ \text{ K} = 4.5^\circ \text{ K}.$$

3.3.4 Temperature increase due to the sidelobes at 45° elevation angle for both radiometers.

(a) For the 35 GHz radiometer.

When tipping the antenna until 45°, temperature increase due to the sidelobes (mentioned in Figure 3.5 (b)) is 3.5°K (see Figure 3.4 Top), and the temperature increase due to other sidelobes (mentioned in Figure 3.5 (a)) is assumed to be constant upon the radiometer. Therefore, the total temperature increase due to the sidelobes is:

$$3.5 + 8.5 = 12^\circ \text{ K}.$$

(b) For the 16 GHz radiometer.

This calculation can be done in the same way as in (a). But there is no temperature increase for the radiometer, even at the zenith angle 45°. Thus, 4.5°K is also the temperature increase due to all the sidelobes. Therefore, the antenna and feeder losses that can be expected are (24* - 12° = 12°K for the 35 GHz radiometer and 35°* - 4.5° = 30.5°K for the 16 GHz radiometer.

4. SKY TEMPERATURE INCREASE DUE TO RAIN AND CLOUD

4.0 General Description

In this section, the sky temperature increase Δ T is defined as being equal to the difference between the temperature of the clear sky, and that of the rainy or cloudy sky. Temperature change due to the change of water vapor content could not be found clearly on the radiometric recording, because data are not plentiful and also the water vapor content did not change greatly during the measurement, over several clear days.

The 35 GHz radiometric temperature sometimes suddenly rose from the clear sky temperature to about 250° - 270°K within 2 or 3 minutes, (8 to 10 minutes for 16 GHz), after which a severe rain storm struck the site. When it is raining, the temperature increase, Δ T, is easily obtained but this temperature increase includes the temperature of the raindrops residual on the protective antenna cover of RF-transparent film.** This latter increase must be taken into consideration for the data obtained during rain.

4.1 Temperature Increase due to Rain

The relation between the 10-minute average temperature increase and the 10-minute average rainfall rate at the receiving point are shown from Figure 4.1 to Figure 4.3. One of these (Figure 4.1) seems to be in good correlation, when it rained uniformly. But most of the rain data (when it rained heavily in summer) showed a time delay for the rain starting; the temperature increased quickly to the highest temperature (near ground temperature) within 5 minutes at 35 GHz, and in 8 minutes at 16 GHz (Figure 4.4).

Considering Figure 4.1 through 4.3, if the rainfall rate is less than 10 mm/hr, correlation seem to be good among theory, the other experimental data, and the measured data, even at a 45° elevation angle. This is of course due to the widespread structure of light rain. In heavy rain, the rain cell is small and usually the measured temperatures at slant angles are less than the calculated ones. This is easily understood as follows.

*See section 3.2.

**This film has been changed to a better one; no residual raindrops cling to it.

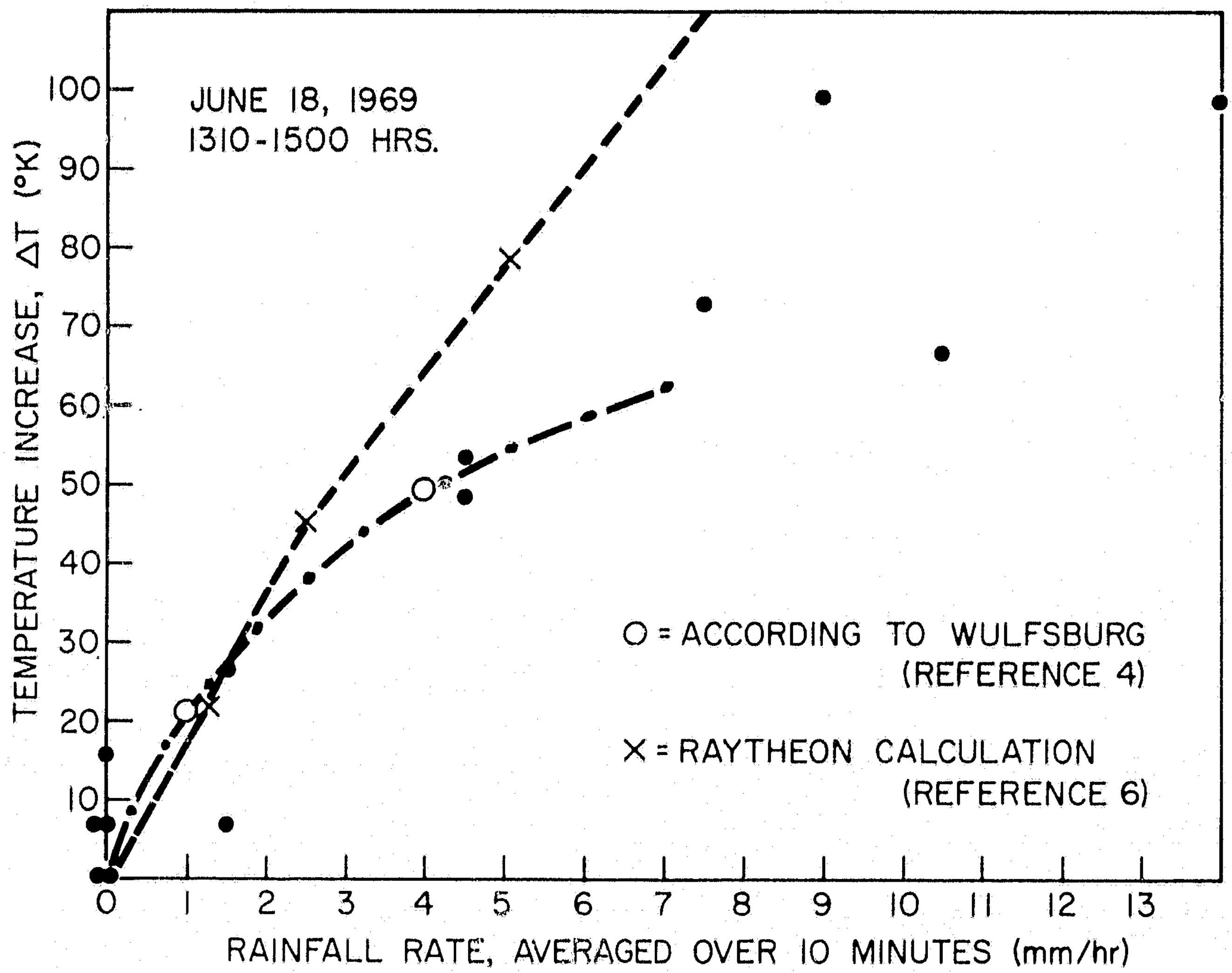

Figure 4.1. Rainfall rate vs. temperature increase for 16 GHz.

In Figure 4.5, Raytheon model (Reference 6) for heavy rain structure shows that point B has a maximum rainfall rate, but the temperature for 45° elevation at point B becomes smaller (about 60% of the vertical loss, for example, at 35 GHz). But in that figure, the slant path loss of 45° elevation becomes largest at line 2, about 80% of the point B vertical loss. As indicated above, this structure shows less temperature in heavy rain, at a certain elevation angle. When thinking of a one-point rainfall and a one-point radiometer temperature measurement, a time delay method would be useful to find the correlation between the measured temperature increase and rainfall rate. If the best correlation could be found, by shifting the time scale of the rain, the time delay could be used to show the storm speed toward the observing point. This is not analyzed here.

4.2 Temperature Increase due to Cloud.

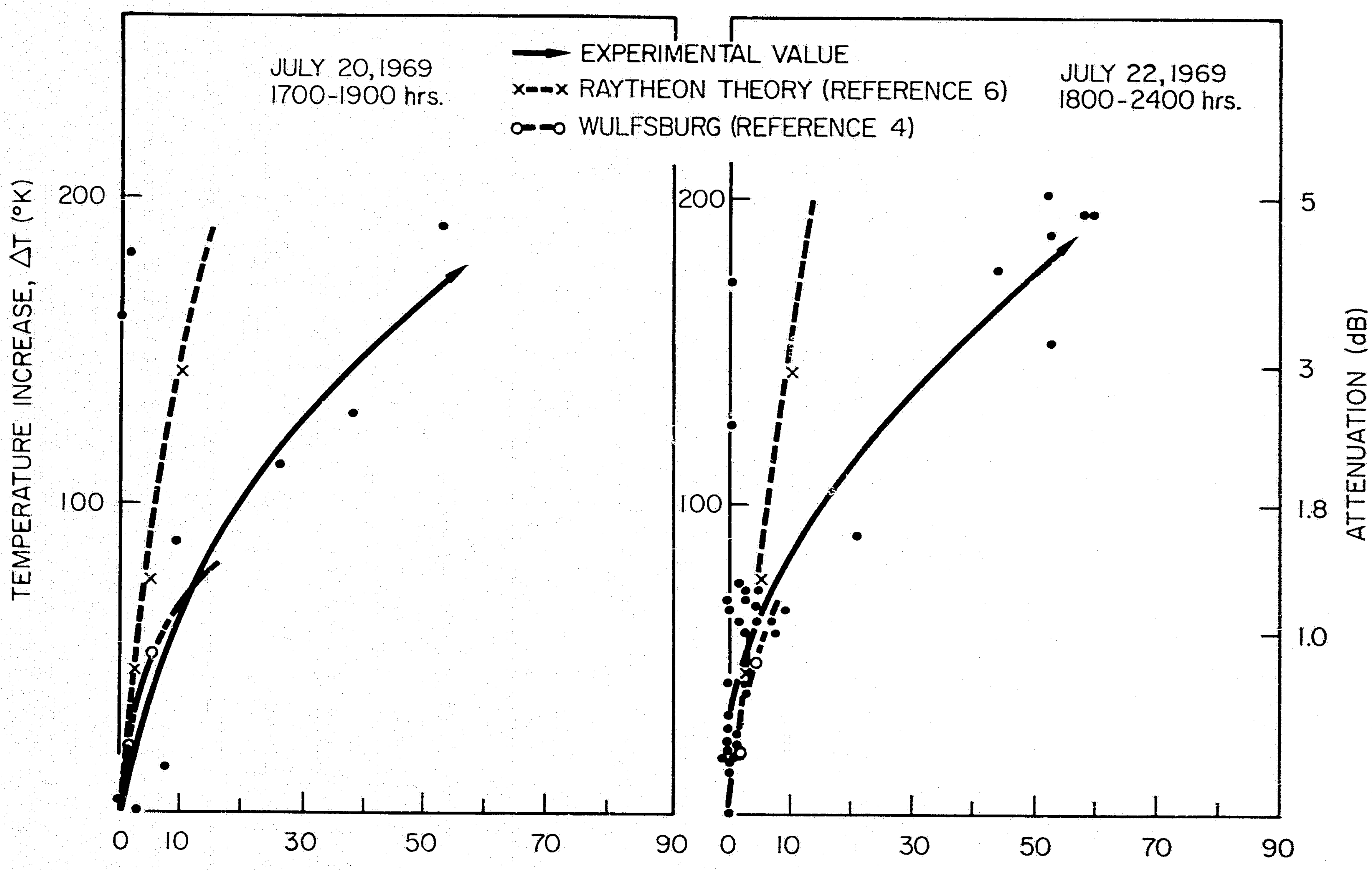

Figure 4.2. Rainfall rate vs. temperature increase for 16 GHz.

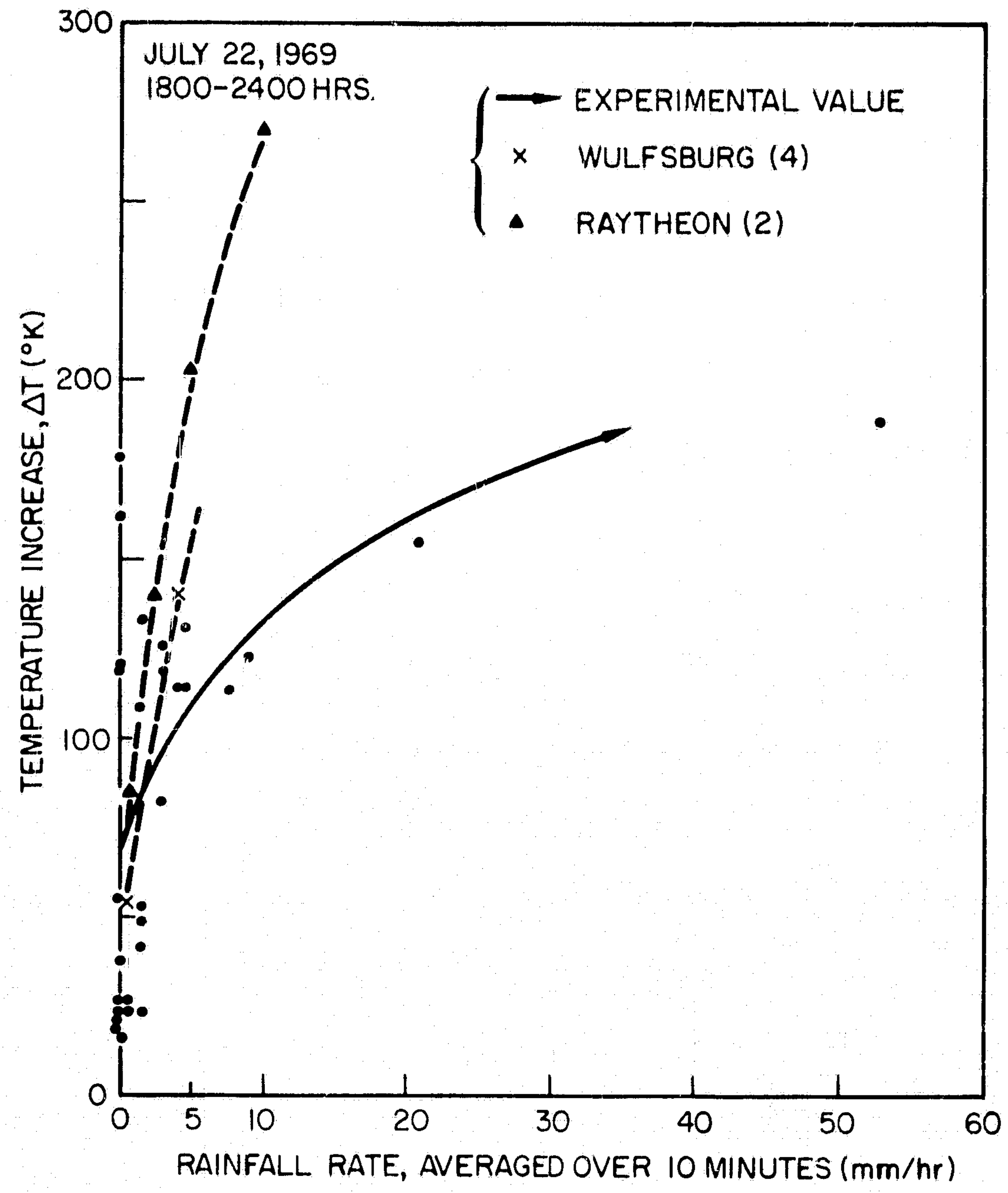

Figure 4.3. Rainfall rate vs. temperature increase for 35 GHz.

4.2.1 Scintillation of cloud.

These radiometers each have an integration time of a second, but scintillations within 1 minute are mostly due to noise fluctuations, and the scintillation period with cloud is usually longer than 1 minute. A 10 minute interval has been chosen for so-called cloud scintillation here. Also, the maximum-to-minimum temperature range within ten minutes has been measured and a comparison has been made between that temperature range for 35 GHz and that for 16 GHz.

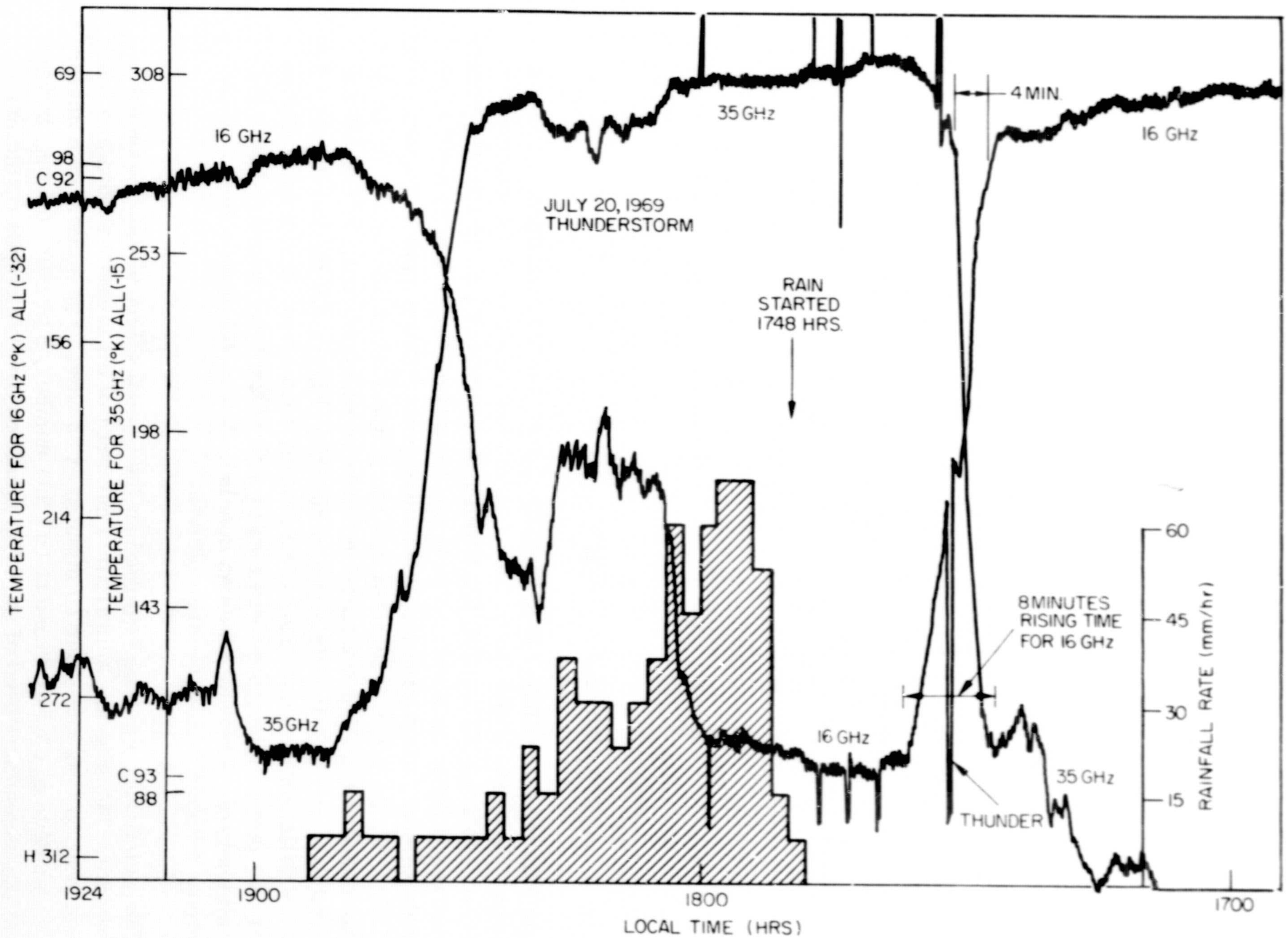

Figure 4.4. Plot of temperature (°K) vs. time for 16 GHz and 35 GHz on July 20. (Shaded area represents rain).

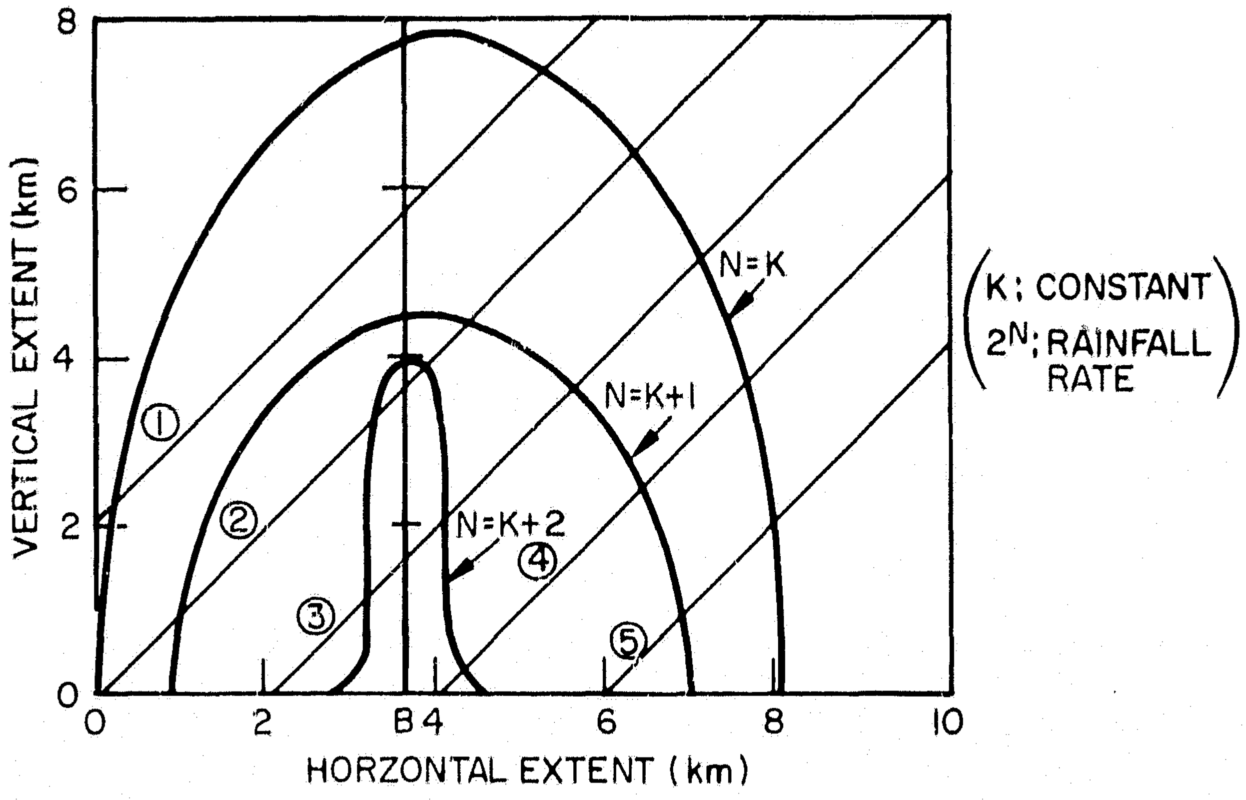

Figure 4.5. One of the Raytheon models; profile of heavy rain structure.

4.2.2.1 Distribution of scintillation numbers

The scintillation number is defined as the number of crossings of the average temperature line within 10 minutes, when cloud intersects the radiometer beams. In Table 4.1 (a) and (b), the scintillation numbers per 10 minutes versus the occurrence time are shown. These numbers were measured at a 45° elevation angle without rain during the experiment period (from June 18 through July 31st, 1969). Table 4.1 is translated into the graph Figure 4.6 (a) and (b) to display the distribution. The scintillation numbers which occur in 90% of all the measured data are 4 at 16 GHz and 5 at 35 GHz. Figure 4.6 (a) and (b) show that larger scintillation numbers than 4 and 5 occur less often. And a scintillation number of 1 per 10 minutes covers almost 40% of the total measured data for both radiometers. Therefore we can conclude that cloud often comes into the radiometer antenna beams in large clumps.

This scintillation can be regarded as the typical effect of cloud upon the radiometers. The average scintillation numbers of all measured data are 2 per 10 minutes at 16 GHz and 3 per 10 minutes at 35 GHz. The 35 GHz radiometer is very sensitive to cloud movement and this number, 3 per 10 minutes, is very close to the ascending speed of the local small convective clouds (cumulus) (Reference 7) for which the temperature increase due to the cloud would occur largely within the main beam.

Table 4.1
Scintillation Number Distribution Within 10 Minutes

(a) For 35 GHz

	Number	Occurrence	Percent	Average Temperature Increase
	1	82	42.2	15.6°K
	2	16	8.2	11.9
	3	29	14.9	13.4
	4	28	14.5	12.1
	5	17	8.8	17.0
	6	6	3.1	13.0
	7	9	4.6	11.5
	8	2	1.0	18.5
	9	1	0.5	13.0
	10	4	2.0	16.3
Weighting Average Scintillation Number		2.4	(100%)	14.3°K Average Increment

(b) For 16 GHz

	Number	Occurrence	Percent	Average Temperature Increase
	1	49	36.0	6.6
	2	39	28.6	4.3
	3	24	17.6	9.5
	4	13	9.6	5.0
	5	3	2.2	6.0
	6	7	5.1	4.7
	7	0	0	0
	8	1	0.7	3.0
Weighting Average Scintillation Number		2.3	(100%)	6.1°K Average Increment

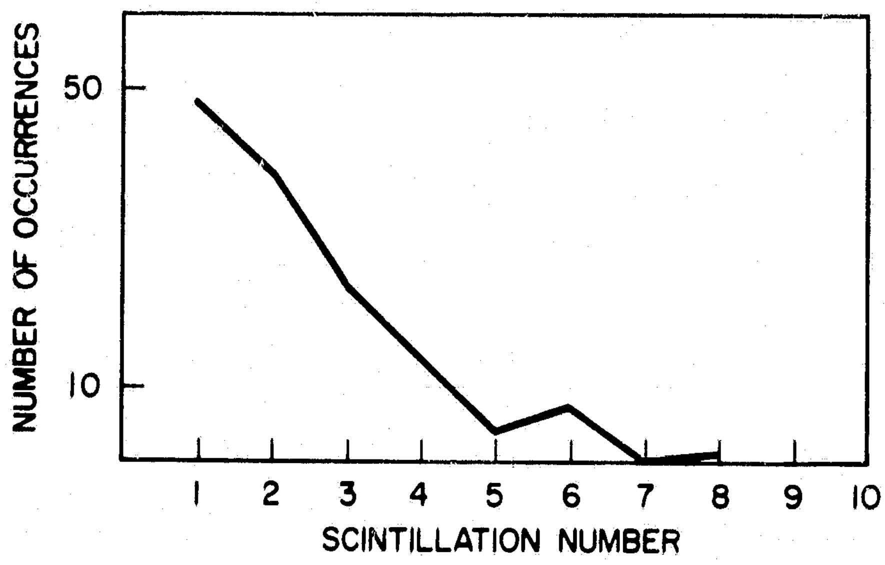

Figure 4.6(a). Scintillation number for 16 GHz.

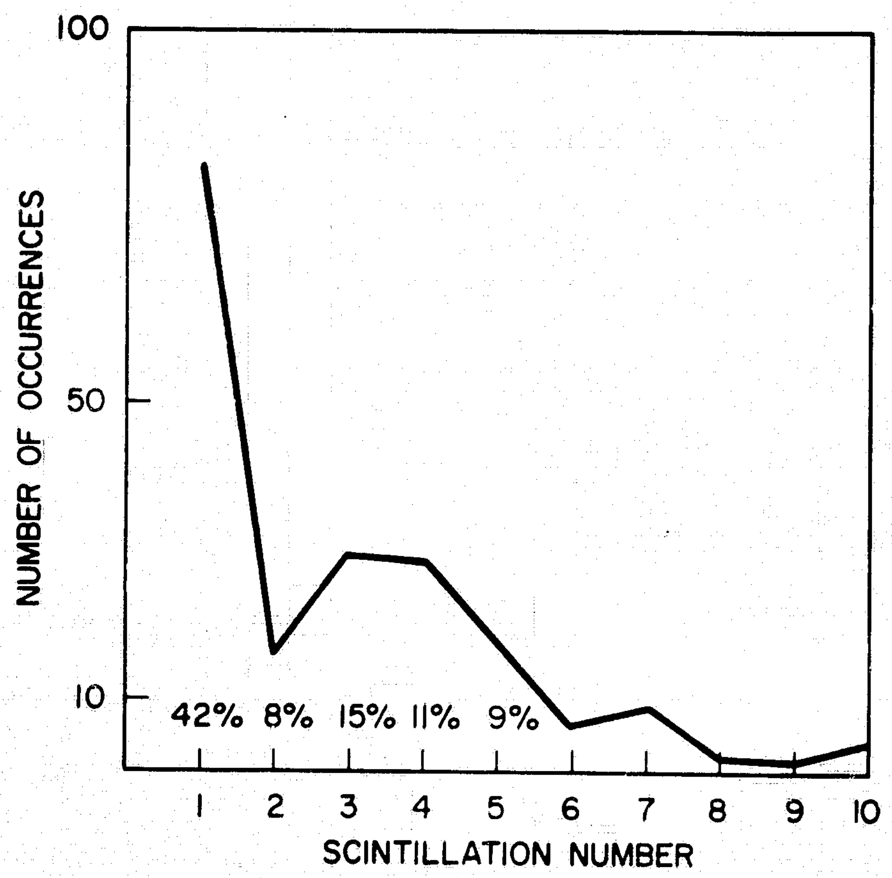

Figure 4.6(b). Scintillation number for 35 GHz.

Table 4.2
Distribution of the Scintillation Number 1 Per 10 Minutes

(a) For 35 GHz

Increment	Number of Occurrences	%	
100 → 100(°K)	1		
90 → 100	0		
80 → 90	1		
70 → 80	1		
60 → 70	2		
50 → 60	2		
40 → 50	0		
30 → 40	1		
20 → 30	9	11%	
10 → 20	21	26%	≈ 90%
0 → 10°K	42	52%	

(b) For 16 GHz

Increment	Number of Occurrences	%
40 → 50 (°K)	0	
30 → 40	1	
20 → 30	2	
10 → 20	1	
0 → 10	45	92%

The average temperature increases with cloud are 6°K at 16 GHz and 14°K at 35 GHz. At 35 GHz, the average temperature increase of 14°K is the middle of the range of data, 5 - 25°K, measured by K. N. Wulfsburg A.F.C.R.L. (Reference 4).

4.2.1.2 Distribution of the scintillation number 1 per 10 minutes

The distribution of the scintillation number 1 per 10 minutes (Table 4.2 (a) and (b)) shows that increases of less than 10°K account for 92% of all the temperature increases with cloud at 16 GHz; and increases of less than 30°K account for 90% of all the increases at 35 GHz. The remaining 10% are caused by rain cloud (Nimbostratus). This measurement was carried out at a 45° elevation angle; at zenith a different distribution would be expected.

4.2.2 Temperature increases due to large clumps of clouds and their duration

This paragraph shows only a partial analysis of the data. The temperature increases due to big clumps of clouds are defined in Figure 4.7. In Table 4.3 an example is shown of the temperature increase ΔT and their duration time Δt for a couple of days in our experiment. These data include the rain clouds for some of which the temperature increases 80°K. If these temperature increases are mainly caused by cumulus (i.e., or local convection) clouds, the longest duration would be 20 to 30 minutes. Longer times than this occur for the case when widely spread rain cloud (Nimbostratus and other clouds) intersects the main beam. No analysis of longer periods is made here.

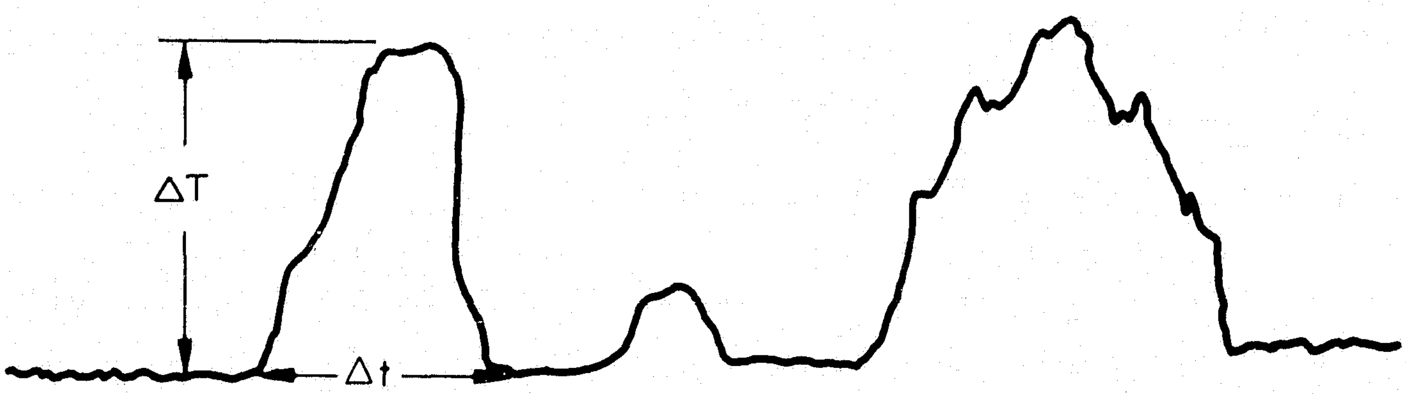

Figure 4.7. Changes of temperature (ΔT) due to clouds.

Table 4.3
Examples of the Temperature Rising Time and the Range of Temperature Increase Due to the Big Lumps of Clouds

Date	35 GHz		16 GHz		Ratio ΔT 35/ΔT 16
	Δt	T(°K)	Δt	T(°K)	
6/13	5.5	19	2	5	3.8
	23	82	16	24	2.9
	7	37	6	10	3.7
	2.5	16	1.5	3	5.3
	4	25	9	19	1.3
	1	10	2	3	3.3
	10	54			
6/18	3	17	4	4	4.3
	1.5	7	2	3	2.3
	3	20	4	7	2.8
6/19	2	7			
	3	7			
	16	46	17	17	2.7
	8.5	13	7	3	4.3
	11	17	7	8	2.1
					Average Ratio 3.2

5. CALCULATION OF SKY TEMPERATURE AND MEAN TEMPERATURE FROM 10 GHZ TO 40 GHZ

5.1 The Calculation Procedures of Sky Temperature

1 -A The attenuation at each one-kilometer height increment was calculated according to the standard atmospheric model (Figure 5.1) and integrated over the whole atmospheric path.

$$\left.\frac{\kappa}{\rho}\right|_{H_2O} = \frac{C_1 \times 10^{-278/T}}{T^{5/2}\,\lambda^2}\left[\frac{\Delta\nu/c}{\left(\frac{1}{\lambda_0}-\frac{1}{\lambda}\right)^2+\left(\frac{\Delta\nu}{c}\right)^2}+\frac{\Delta\nu/c}{\left(\frac{1}{\lambda_0}-\frac{1}{\lambda}\right)^2+\left(\frac{\Delta\nu}{c}\right)^2}\right]+\frac{C_2\,\Delta\nu/c}{T\,\lambda^2} \tag{5.1}$$

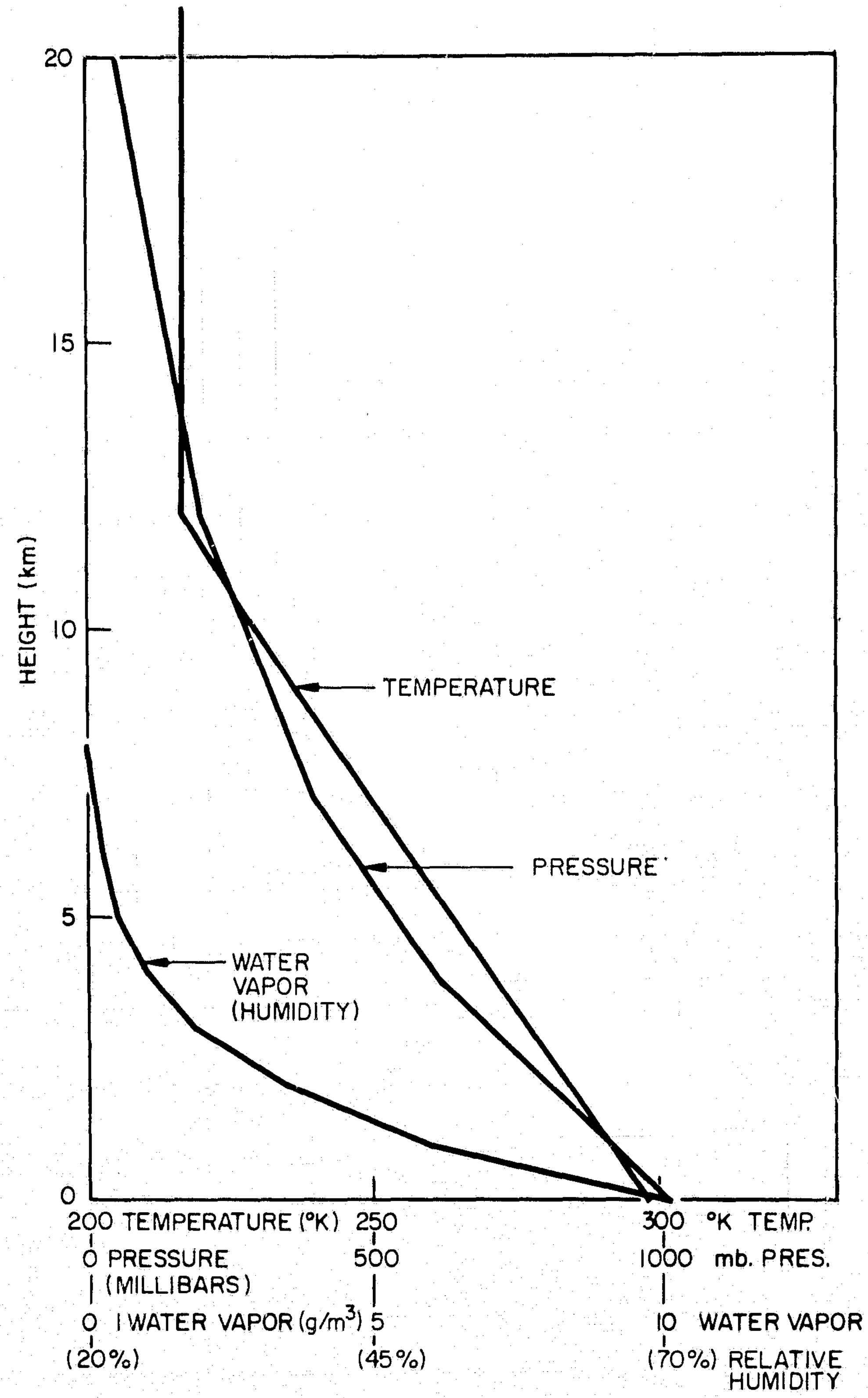

Figure 5.1. Model of standard atmosphere (Reference 3).

κ : attenuation dB/m

$C_1 = 4.77 \times 10^4$

$\Delta\nu/c = 1.51 \times 10^{-3}\ (P + 3.7e)\ T^{-1/2}$ (P, e in mb, T in K°)

$C_2 = (0.207\,\rho + 14.4)$, ρ : Water vapor content g/m³

$\lambda_0 = 1.349$ cm

P : atmospheric pressure,

e : water vapor pressure

T : temperature (°K) at certain height

$$\frac{\kappa}{\rho}\Big|_{O_2} = \frac{0.358}{T\lambda^2}\left[\frac{\Delta\nu/c}{\left(\frac{1}{\lambda_0}-\frac{1}{\lambda}\right)^2+\left(\frac{\Delta\nu}{c}\right)^2}+\frac{\Delta\nu/c}{\left(\frac{1}{\lambda_0}+\frac{1}{\lambda}\right)^2+\left(\frac{\Delta\nu}{c}\right)^2}+\frac{\Delta\nu/c}{\left(\frac{1}{\lambda}\right)^2+\left(\frac{\Delta\nu}{c}\right)^2}\right] \qquad (5.2)$$

κ : in dB/km

ρ : is the oxygen density g/m³

$\Delta\nu/c = 3.38 \times 10^{-4}\ P \cdot T^{-1/2}$ (c; velocity of light)

$= 0.02$ (T = 293°K, P = 1013 mb)

$\lambda_0 = 0.5$ cm

Equations (5.1) and (5.2) used by Shulkin (Reference 1) were originally derived by Van Vleck (References 8, 9, 10).

(2) T_m and T_s are calculated as follows:

$$T_m = \frac{\int_0^{\tau_0} T e^{-\tau}\, d\tau}{1 - e^{-\tau_0}} \qquad (5.3)$$

$$T_s = (1 - \alpha) \cdot T_m \qquad (5.4)$$

T_m : mean temperature

T_s : sky temperature

T : temperature at certain height

τ_0 : total attenuations in dB.

τ : attenuation up to certain height

$\alpha = e^{-\tau_0}$ fractional transmission coefficient, in Neper

For zenith angle larger than zero, secant ϕ law comes into the equation (4.4). Therefore we have to replace τ for τ sec ϕ.

$$\tau \to \tau \text{ secant } \phi, \quad \phi \text{ in zenith angle}$$

$$T_s = (1 - e^{-\tau_0 \text{ secant } \phi})\, T_m$$

$$= (1 - \alpha^{\text{secant } \phi})\, T_m \tag{5.5}$$

③ Computations were carried out for T_m and T_s under various ground conditions and several atmospheric precipitation models. See following paragraphs. For reference, another calculation was carried out, as follows.

①-B Next, equations of Bean and Dutton (Reference 2) were used for another calculation of atmospheric attenuations at the same frequencies as mentioned in ① -A and the results were compared with those of the method written in ① -A in this section.

$$\frac{\kappa}{\rho}\bigg|_{H_2O} = \frac{3.53\times 10^{-3}}{\lambda^2}\left[\frac{\Delta\nu/c}{\left(\frac{1}{\lambda_0}-\frac{1}{\lambda}\right)^2+\left(\frac{\Delta\nu}{c}\right)^2}+\frac{\Delta\nu/c}{\left(\frac{1}{\lambda_0}+\frac{1}{\lambda}\right)^2+\left(\frac{\Delta\nu}{c}\right)^2}\right]\left(\frac{293}{T}\right)^{2.5}$$

$$+\frac{0.05}{\lambda^2}(\Delta\nu/c)\cdot\left(\frac{293}{T}\right) \tag{5.6}$$

$$\Delta\gamma/C = 0.087 \times \left(\frac{P}{1013.25}\right)\left(\frac{318}{T}\right)^{1/2}(1 + 0.0046\,\rho)$$

$$\kappa\Big|_{O_2} = \frac{0.34}{\lambda^2}\left[\frac{(\Delta\nu/c)_1}{\left(\frac{1}{\lambda_0}-\frac{1}{\lambda}\right)^2+\left(\frac{\Delta\nu}{c}\right)_1^2}+\frac{(\Delta\nu/c)_1}{\left(\frac{1}{\lambda_0}+\frac{1}{\lambda}\right)^2+\left(\frac{\Delta\nu}{c}\right)_1^2}+\frac{(\Delta\nu/c)_2}{\left(\frac{1}{\lambda}\right)^2+\left(\frac{\Delta\nu}{c}\right)_2^2}\right]\times\left(\frac{293}{T}\right) \quad (5.7)$$

at Ground

$$(\Delta\nu/c)_1 = 0.018\,(P/1013.25)\,(293/T)^{0.75}$$

$$(\Delta\nu/c)_2 = 0.049\,(P/1013.25)\,(293/T)^{0.75}$$

$$P_{O_2} = 0.210 \times P \quad (P\text{: atmospheric pressure})$$

$$\rho_{O_2} = 0.385 \cdot \frac{P_{O_2}}{T} \quad (P_{O_2}\text{: partial pressure of oxygen})$$

Therefore, the density of O_2 changes as a function of P/T. For the calculation of oxygen attenuation at various heights, (P/T) must be multiplied by (5.7). A slight calculation difference was found between the value of $\Delta\nu/c$ calculated by (5.2) and by (5.1) when both calculations were carried out for oxygen.

5.2 Mean Temperature Calculation

The mean temperature, T_m, was calculated by converting vertical loss (Reference 3) into sky temperature; and T_s is derived from T_m. The T_m changes were computed by using (5.3) and (5.5) under various frequencies, ground conditions and also for several zenith angles.

Calculated mean temperatures are shown in Figure 5.2. The T_m values were calculated between 10 GHz and 40 GHz, at constant temperature T_g = 288°K on the ground; the maximum T_m differences with changing humidity are 8°K.

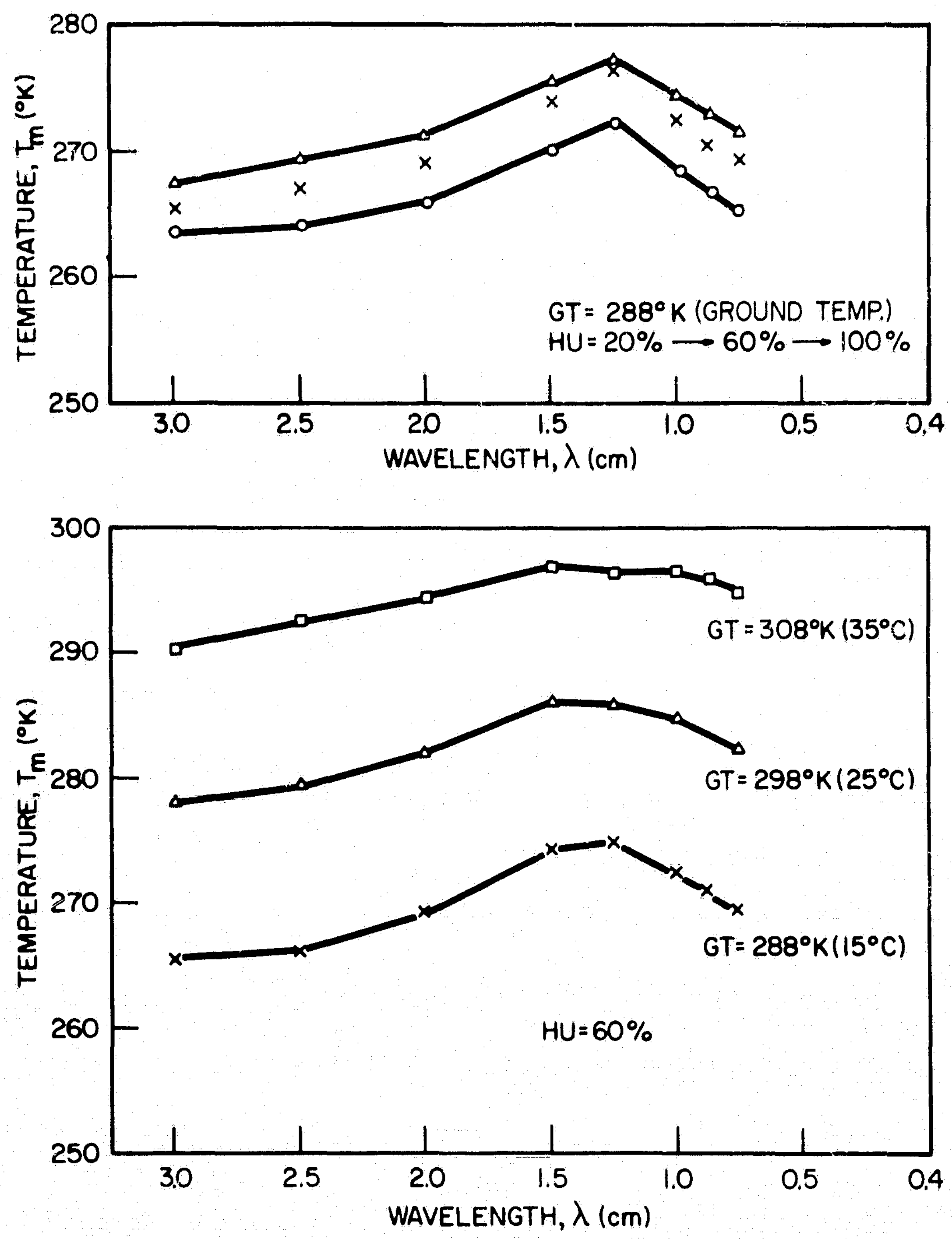

Figure 5.2. T_m change due to ground condition.

Therefore, when T_s is calculated with T_m derived from ground temperature (for example, $T_m = 1.12\ T_g - 50$) (Reference 4) α must be larger than 0.8, if the permissible error is $\Delta T_s \leq 2°K$. A simple calculation follows:

$$T_s = (1 - \alpha) \cdot T_{m_1}, \tag{5.8}$$

$$T_s' = (1 - \alpha) \cdot T_{m_2}, \tag{5.9}$$

where

T_{m_1} is derived from ground temperature, and

T_{m_2} includes the effect of humidity.

Then

$$T_s - T_s' = \Delta T_s = (1 - \alpha)\ (T_{m_1} - T_{m_2}) \leq 2;$$

and

$$\text{if } T_{m_1} - T_{m_2} = 8, \text{ then } \alpha \geq 0.75.$$

In one of the frequencies, the range of T_m due to humidity changes is about 4°K, so α must be larger than 0.5, calculated in the same way as above.

In case of changing ground temperature T_g, the change in T_m is proportional to this change in T_g, ground temperature, as has been shown also by Wulfsburg (Reference 4). A comparison of the Wulfsburg results, $T_m = 1.12\ T_g - 50$, with our computed values shows fairly good agreement for frequencies larger than 10 GHz (Figure 5.3).

The mean temperature also varies only slightly with zenith angle ϕ at all frequencies calculated (Tables (5.6) and (5.7)). Therefore, there is no problem in calculating T_s at about 40° elevation angle (for satellite data acquisition).

5.3 Calculation Results for Clear Days, Using Shulkin's Method

In Figure 5.4 is shown the range of variation in sky temperature due to water vapor (humidity) changes and also due to ground temperature changes. For a constant ground temperature of 288°K, the sky temperature varies from 3 to

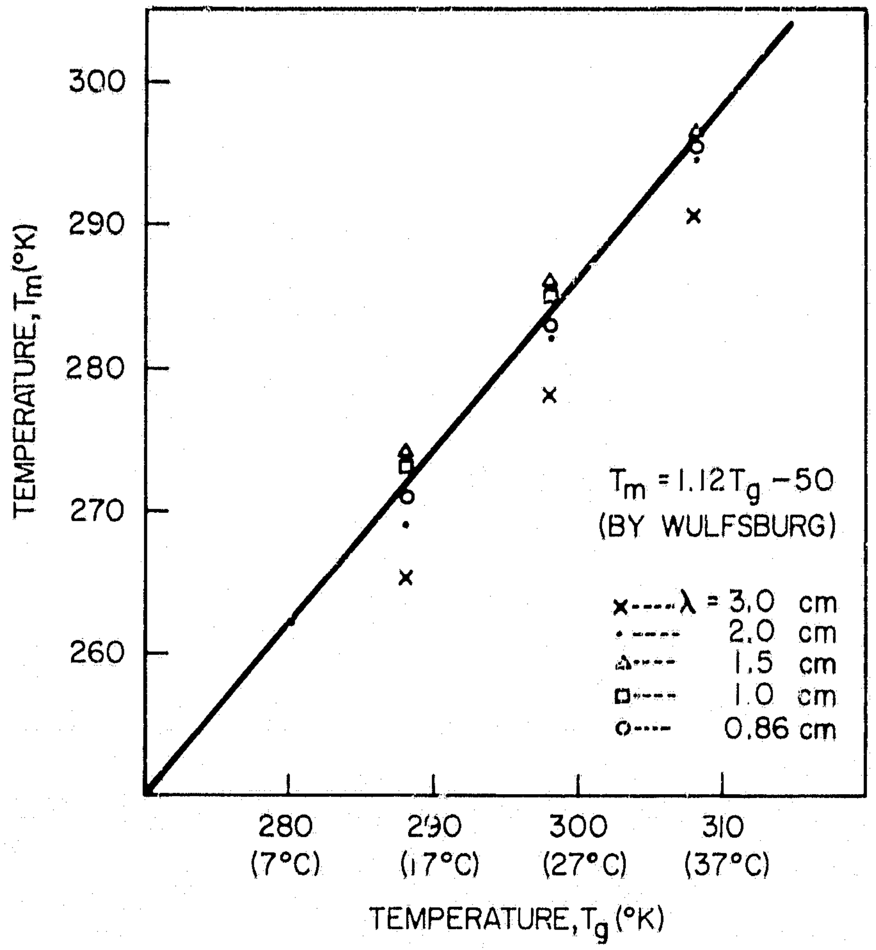

Figure 5.3. T_m in the function of T_g (ground temperature).

5.5°K at 15* GHz, and 8 to 18°K at 35 GHz. And under constant humidity, sky temperatures change from 4°K to 8°K for 15* GHz, and 13 to 27°K for 35 GHz.

Near the water vapor resonance peak, $\lambda \approx 1.25$ cm, the sky temperature varies greatly, from 9° to 32°K for constant ground temperature $T_g = 288$°K and from 21° to 57°K for a constant relative humidity of 60%. The sky temperature ranges with changing T_g and humidity are listed in Tables 5.1 and 5.2. The values in Table 5.2 were calculated by the method of Bean and Dutton (Reference 2). For frequencies below 30 GHz, both calculations are in fairly good agreement, but above 30 GHz there exists a difference of nearly 10°K at lowest humidity. These differences are due mainly to the use of the oxygen calculation method.

*This is referred to 16 GHz. Calculation was done at 15 GHz; almost no difference exists.

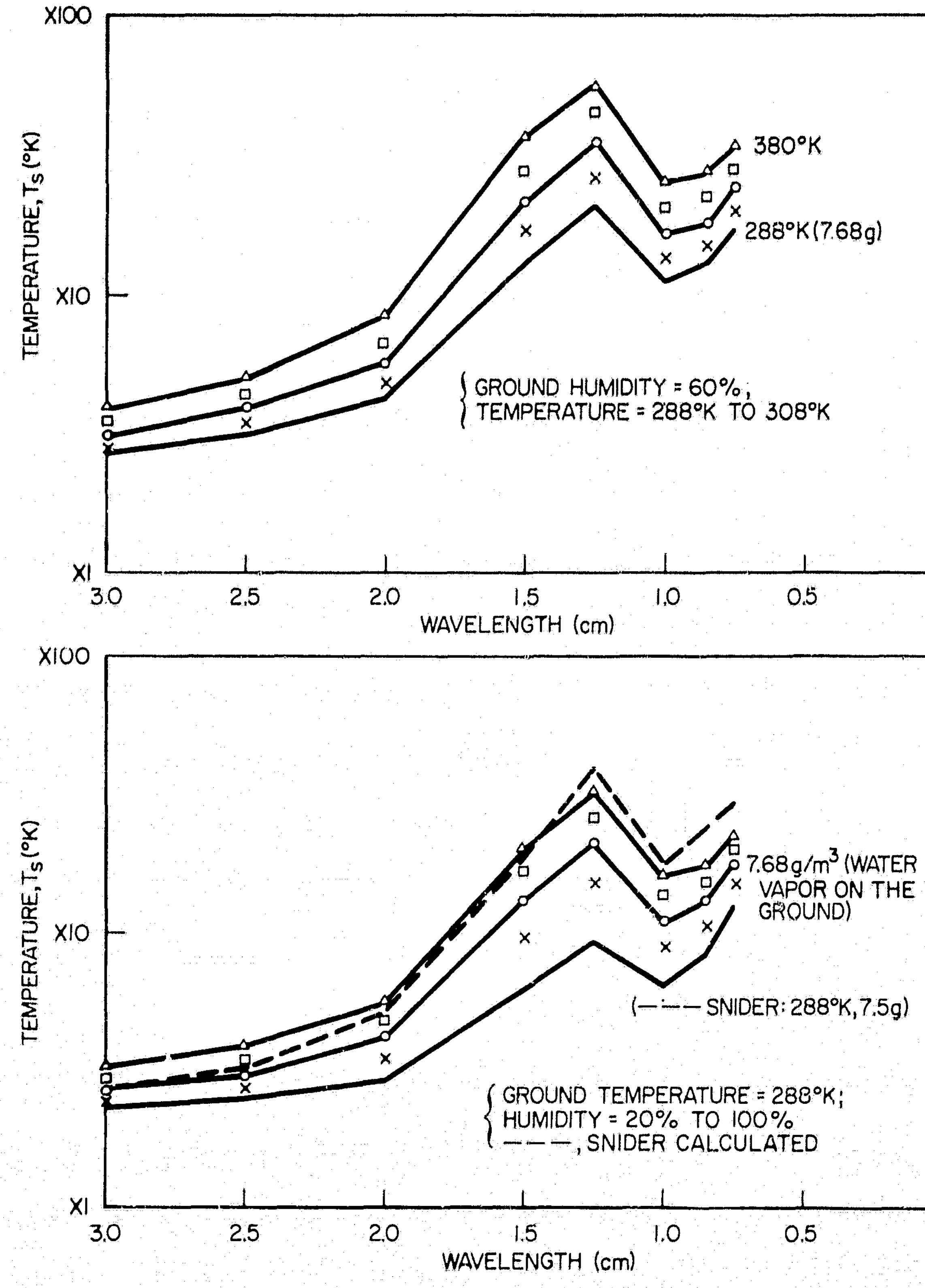

Figure 5.4. Temperature change due to atmospheric conditions (by Shulkins).

Table 5.1
Sky Temperature Variations by the Method of Shulkins (Reference 1). No cloud.

Frequency (GHz)		10	15	20	30	35	40
T_g (°K)	Wavelength, λ (cm) / Humidity 20%/100% (g/m³)	3	2	1.5	1.0	0.8	0.75
		Sky Temperature Increment (°K)					
288	2.6 13.0	2.3 3.1	2.9 5.5	6.2 20.1	6.5 26.1	8.3 17.5	12.7 23.1
293	3.4 17.2	2.3 3.4	3.1 6.7	7.4 26.2	7.2 20.3	8.9 21.6	13.2 27.7
298	4.6 23.0	2.3 4.0	3.3 8.3	9.0 34.2	8.1 26.1	9.7 27.3	14.1 34.1
303	6.0 30.3	2.4 4.6	3.6 10.4	11.1 44.3	9.3 33.7	10.8 35.0	15.2 42.7
308	7.9 39.6	2.5 5.6	4.0 13.4	13.7 56.9	10.9 44.0	12.3 45.4	16.8 54.6

In the graph (Figure 5.5 (a) to (d)), the temperature increment due to the water vapor content can easily be found for the quasi-millimeter and millimeter wavelength regions. Thus if the ground temperature and humidity are known the sky temperature can be obtained easily from Figure 5.5.

In Table 3.3 the "Reference" column shows the expected true temperature by the method of Shulkin (Reference 1) and that of Bean and Dutton (Reference 2). It would be anticipated that the latter method would give nearly the same value as that of Column 4 (in Table 3.3), which has been converted into expected temperature from the experimental value of Reference 1. Below 16 GHz, no sky temperature difference between two methods of calculation can be found.

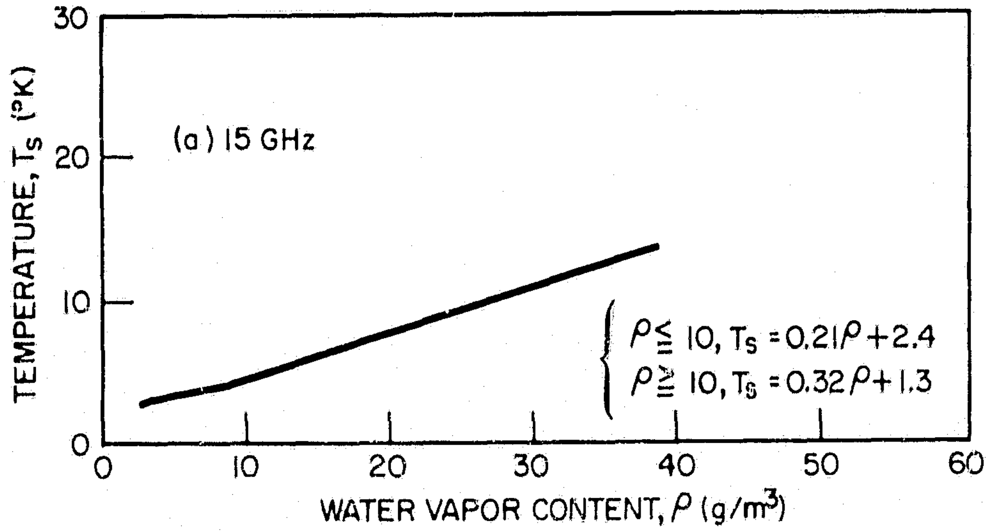

Figure 5.5(a). Sky temperature increase due to water vapor for 15 GHz (Reference 4).

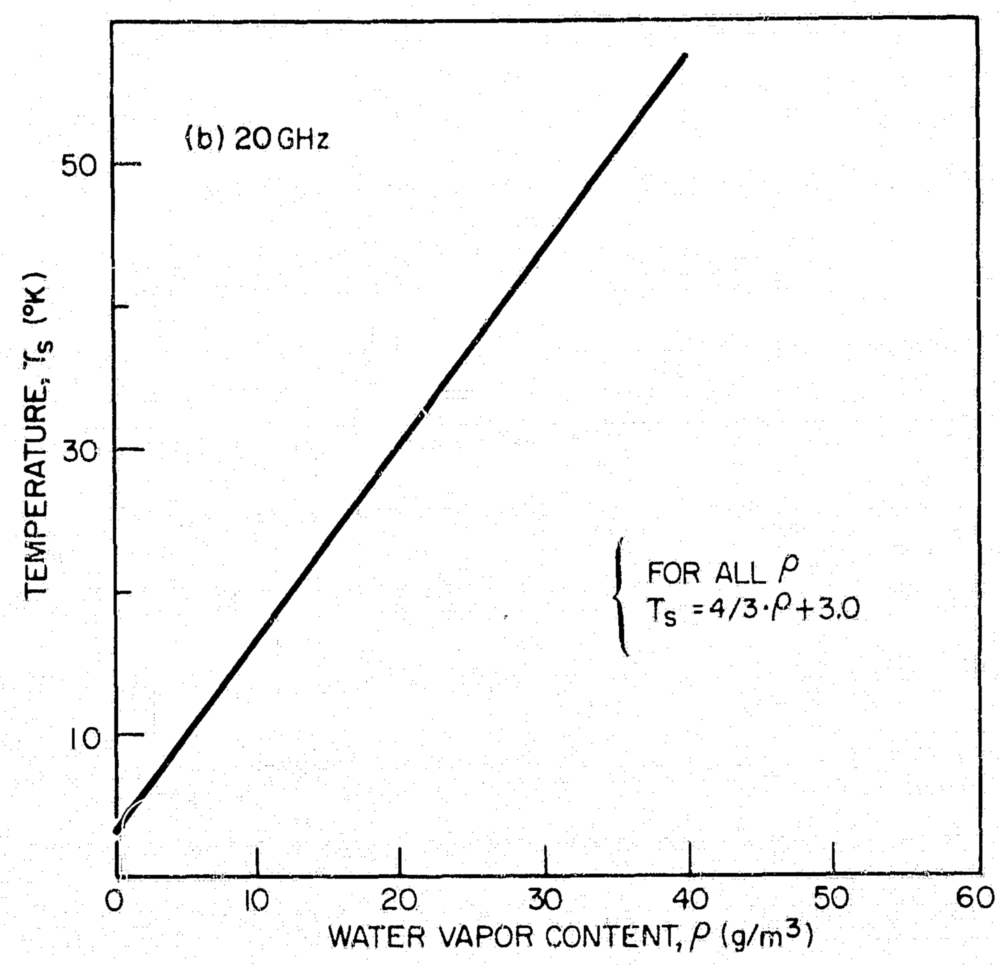

Figure 5.5(b). Sky temperature increase due to water vapor for 20 GHz (Reference 4).

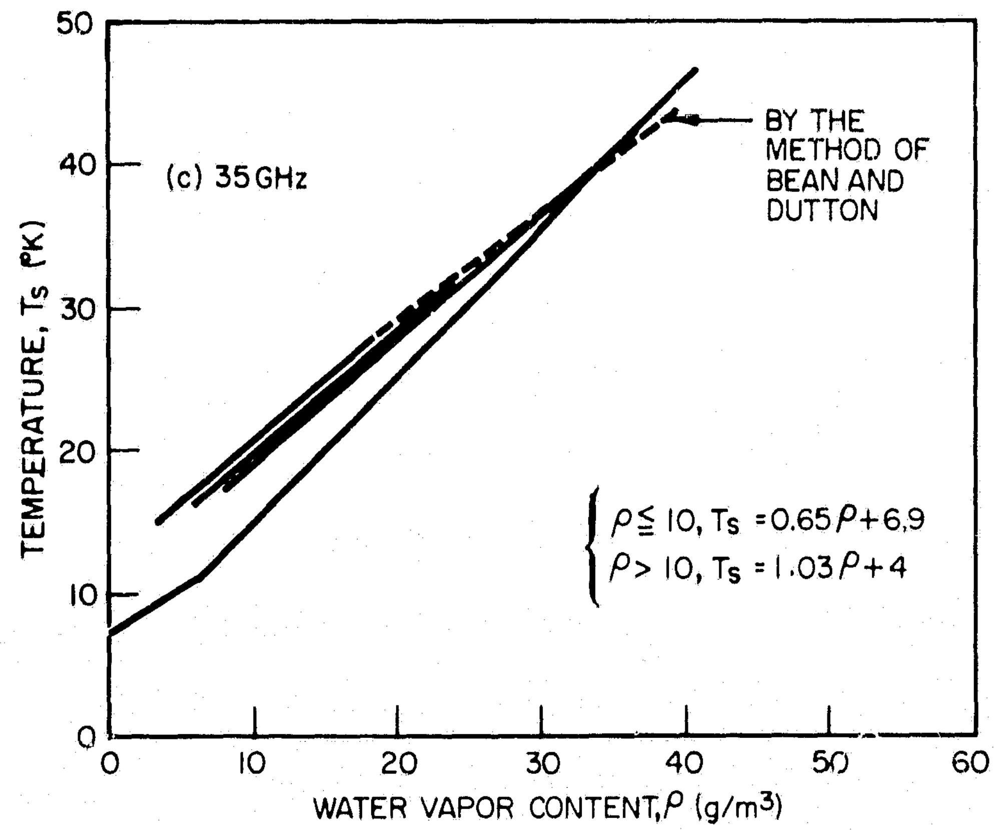

Figure 5.5(c). Sky temperature increase due to water vapor for 35 GHz (Reference 4).

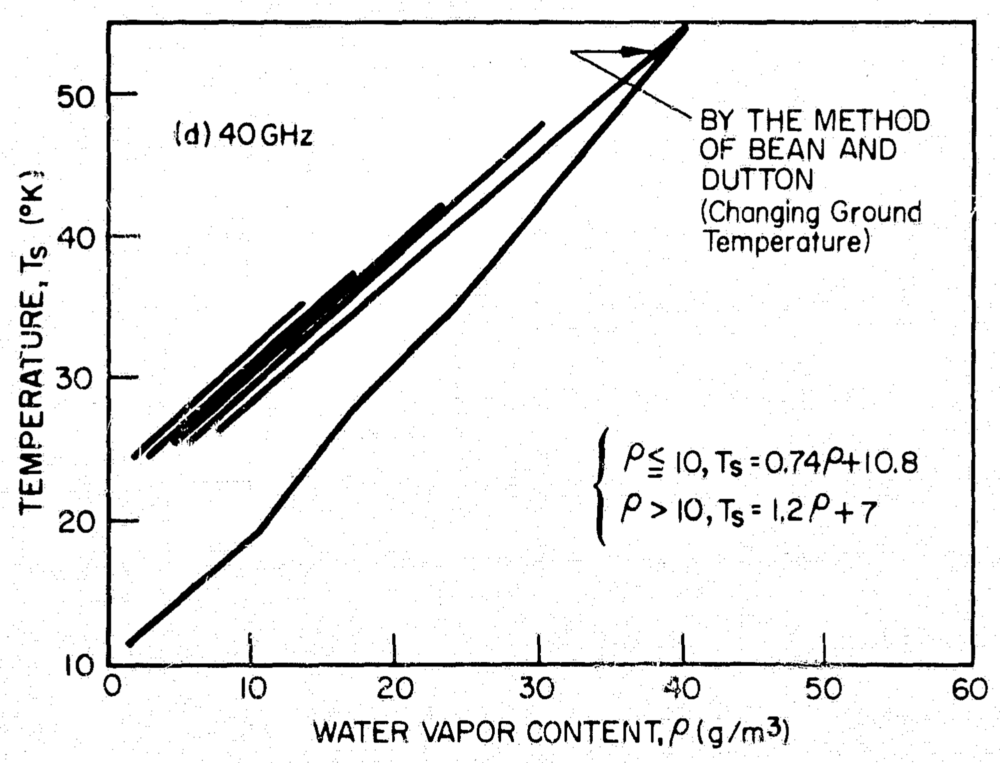

Figure 5.5(d). Sky temperature increase due to water vapor for 40 GHz (Reference 4).

Table 5.2
Sky Temperature Variations by the Method of Bean and Dutton (Reference 2).
No Cloud.

Frequency (GHz)		10	15	20	30	35	40
T_g (°K)	Wavelength, λ (cm) / Humidity, 20%/100% (g/m^3)	3	2	1.5	1.0	0.86	0.75
		Sky Temperature Increment (°K)					
288	2.6 13.0	2.4 3.2	3.3 5.9	7.3 22.0	9.8 19.3	14.4 23.2	24.7 34.2
293	3.4 17.2	2.4 3.4	3.4 6.9	8.3 27.5	10.4 22.9	14.7 26.4	24.8 37.5
298	4.6 23.0	2.4 3.8	3.6 8.2	9.8 34.5	11.1 27.6	15.3 30.8	25.2 42.1
303	6.0 30.3	2.4 4.3	3.8 9.9	11.5 42.8	12.1 33.5	16.1 36.4	25.8 48.1
308	7.9 39.6	2.5 5.0	4.2 12.1	13.7 52.9	23.4 41.1	17.2 43.6	26.9 55.8

Table 5.3 gives a conversion of the sky temperature range of Table 5.1 and 5.2 into the loss in dB along the vertical path and shows how the vertical losses change with ground temperature and humidity. Also, the NASA reference values from Reference 11 are listed in Table 5.4.

The values of Table 5.4 are distributed from 0.13 dB to 0.6 dB. This may be explained by the calculated values, from 0.14 dB to 0.7 dB, when ground temperature and humidity change, as shown in Table 5.3. Attenuation data, calculated by the method of Bean and Dutton (Reference 2), are also shown in columns 4 and 6 of Table 5.3. The value from Bean and Dutton is 0.1 dB larger than the values by Shulkin's method for the lower humidity, as indicated earlier.

Table 5.3
Vertical Loss in dB

Ground Temperature T_g (°K)	Absolute Humidity (g/m^3)	15* GHz		35 GHz	
		Shulkin (Reference 1)	Bean & Dutton (Reference 2)	Shulkin	Bean & Dutton
288	2.56 (20%) ↓ 12.8 (100%)	0.05 dB ↓ 0.09	0.05 dB ↓ 0.096	0.14 dB ↓ 0.29	0.24 dB ↓ 0.39
293	3.4 ↓ 17.2	0.05 ↓ 0.105	0.055 ↓ 0.109	0.14 ↓ 0.35	0.24 ↓ 0.44
298	4.6 ↓ 23.0	0.05 ↓ 0.13	0.056 ↓ 0.127	0.15 ↓ 0.44	0.25 ↓ 0.50
303	6.06 ↓ 30.3	0.055 ↓ 0.16	0.06 ↓ 0.15	0.17 ↓ 0.55	0.25 ↓ 0.58
308	7.9 ↓ 39.6	0.06 ↓ 0.2	0.06 ↓ 0.18	0.29 ↓ 0.71	0.27 ↓ 0.69

*Calculation was carried out at 15 GHz.

5.4 Temperature Increase due to Cloud

Figure 5.6 is also found in the paper of Altshuler et al. (Reference 3). This model was used to calculate the temperature increase due to cloud. Attenuation constants for four frequencies at nearly 0°C are also found in the paper of Gunn and East (Reference 12). Calculations were carried out only for the frequencies for which 0°C attenuation constants are given.

In the calculation for the temperature increase due to cloud, ice cloud attenuation was neglected, because the loss due to ice cloud is two orders of magnitude less than that due to water cloud (Table 5.5). When T_m is calculated, the following formula must be used (Reference 5):

Table 5.4
Measurement List From T. N. Report (Reference 11)

(cm)	Vertical Att. (dB)	Experimenters
2	0.06 - 0.1	Wulfsburg (Radio Science, Vol. 2, p. 319, 1967)
0.87	0.363	Aarons, Barron (IRE, Vol. 46, p. 325, 1958)
0.86	0.22 - 0.32	Wulfsburg (Radio Sci., Vol. 2, p. 319, 1967)
0.86	0.13 - 0.34	Kalagham and Albertini (AFCRL, 1965)
0.86	0.2	Copeland and Tylor (Astrophy. J., Vol. 139, p. 407, 1964)
0.86	0.18 - 0.39	Gibson (IRE, Vol. 46, p. 280, 1958)
0.86	0.2 - 0.6	Gibson (Astrophy. J., Vol. 137, p. 611, 1963)
0.85	0.15 - 0.18	Lymn, Meeks (Astron. J., 69, p. 65-67, 1964)

Table 5.5
Attention Due to Precipitation and Cloud

Condition of Atmosphere	Wavelength, λ (cm)	3.2	1.8	1.24	0.9
Rain	Attenuation, DB/km	$0.0074\ R^{1.31}$	$0.045\ R^{1.14}$	$0.12\ R^{1.05}$	$0.22\ R^{1.00}$
Water cloud (0°C) (10°C)	M water content,	8.58×10^{-2} M 6.3×10^{-2} M	26.7×10^{-2} M 17.9×10^{-2} M	53.2×10^{-2} M 40.6×10^{-2} M	99×10^{-2} M 68.1×10^{-2} M
Ice cloud (-10°C) (-20°C)	M (g/m^3)	8.19×10^{-4} M 5.63×10^{-4} M	14.6×10^{-4} M 10×10^{-4} M	21.1×10^{-4} M 14.5×10^{-4} M	29.3×10^{-4} M 20.0×10^{-4} M

$$T_{sKT} = T_s\, \alpha + (1 - \alpha)\, T_{m_c} \tag{5.10}$$

where

T_{sKT}: total sky temperature

α: loss integrated to the height of 3 km

T_s : sky temperature above 3 km

T_{m_c} : T_m with cloud, from ground to 3 km.

This equation is also used for the calculation when including rain. Figure 5.7 shows the temperature increase due to cloud, calculated by equation (5.10). The temperature increase due to water content is much more prominent in the millimeter wave frequencies. For example:

Temperature Increase ΔT

	No Cloud	1g water Cloud
λ = 1.8 cm:	7°K	23°K
λ = 0.9 cm:	15°K	68°K

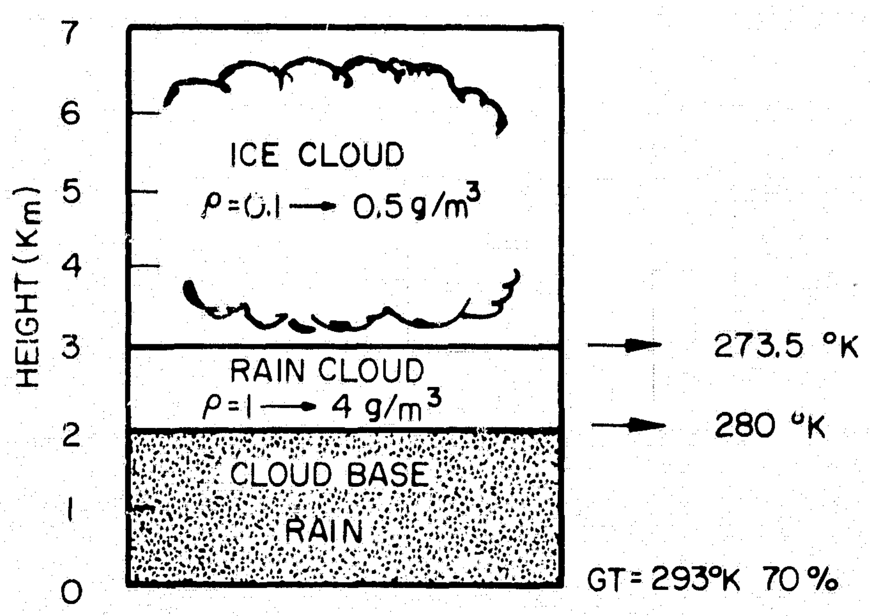

Figure 5.6. Model of atmosphere with precipitation.

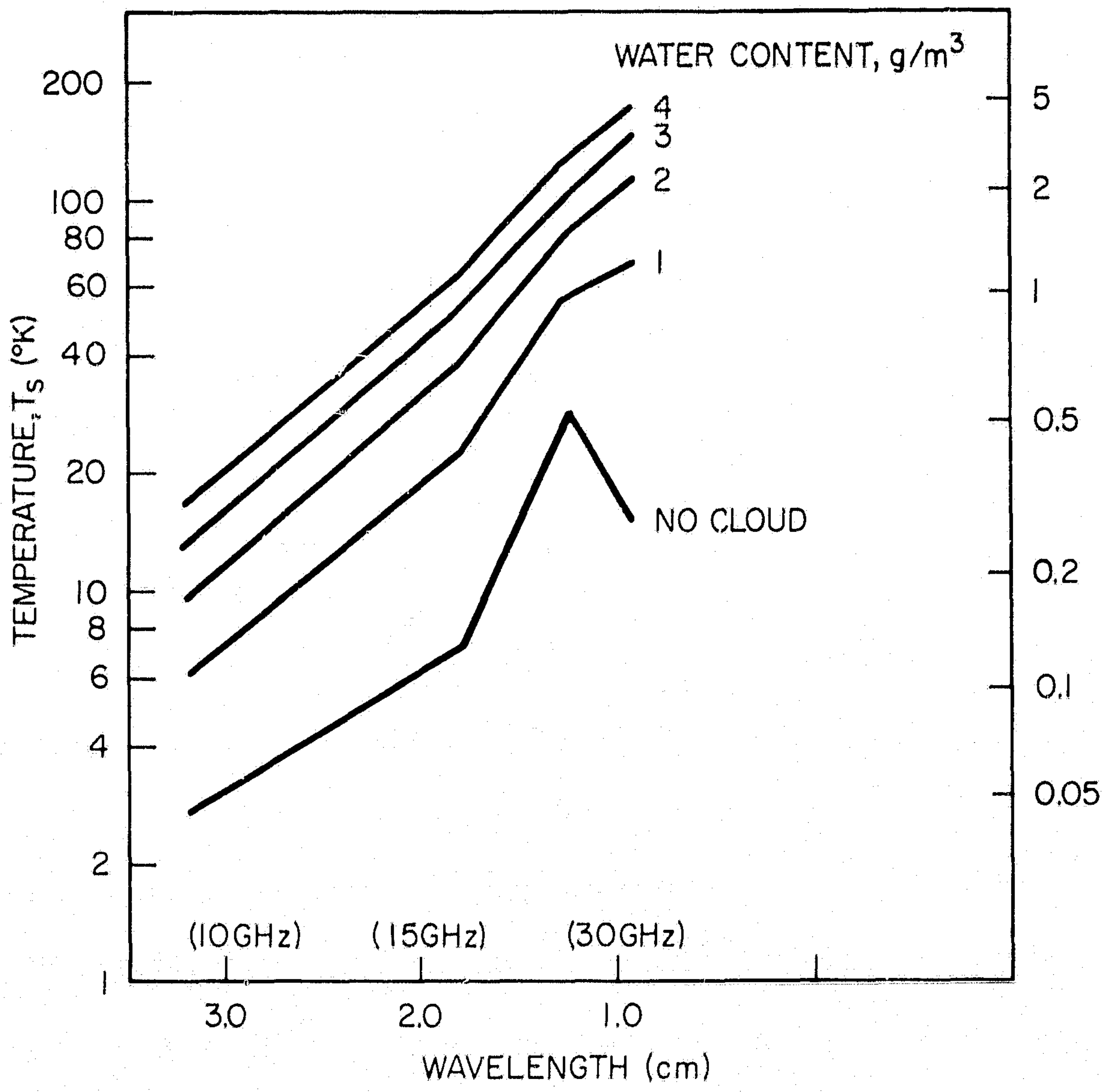

Figure 5.7. Temperature increase due to water cloud.

Next are shown the calculated data sheets for reference. Table 5.6 (a) to (e), Figure 5.8, Table 5.7 (a) to (e) and Figure 5.9 show zenith angle versus the sky temperatures (T_{sKT}), the atmospheric loss (α, TAOSS) and T_m when the sky contains rain clouds from 2 km to 3 km (Figure 5.6). TMG and TSG were calculated from all the losses including atmospheric and cloud loss. T_{sKT} and TSG seem to have the same value because T_s is much smaller than TMC, the cloud mean temperature (T_{m_c} in the equation (5.10)).

5.5 Temperature Increase due to Rain and Rain Attenuation in dB

When it is raining, the vertical structure in Figure 5.6 can be assumed. The attenuations for rain and nearly 0°C cloud are also listed in Table 5.5. The ground temperature and the relative humidity are 293°K and 70% respectively.

Table 5.6–Calculated Data Used for Figure 5.8 ($\lambda \approx 1.8$ cm. (16 GHz), GT = 293°K, R.H. = 70%)

(a) CLOUD WATER = 0.0, RAIN 0.0

DEGREE		TM		TS		TAOSS,DB		TMG
0.0		255.694		1.638		0.112		278.200
	ALPHA=	0.981	TMC=	285.723	TSKT=	7.078	TSG=	7.113
5.00		255.694		1.644		0.113		278.201
	ALPHA=	0.981	TMC=	285.723	TSKT=	7.105	TSG=	7.140
10.00		255.694		1.663		0.114		278.202
	ALPHA=	0.981	TMC=	285.724	TSKT=	7.185	TSG=	7.222
15.00		255.695		1.694		0.116		278.204
	ALPHA=	0.980	TMC=	285.724	TSKT=	7.323	TSG=	7.361
20.00		255.696		1.740		0.120		278.207
	ALPHA=	0.980	TMC=	285.725	TSKT=	7.524	TSG=	7.564
25.00		255.696		1.803		0.124		278.211
	ALPHA=	0.979	TMC=	285.727	TSKT=	7.796	TSG=	7.838
30.00		255.699		1.885		0.130		278.217
	ALPHA=	0.978	TMC=	285.728	TSKT=	8.152	TSG=	8.198
35.00		255.701		1.990		0.137		278.223
	ALPHA=	0.977	TMC=	285.730	TSKT=	8.609	TSG=	8.660
40.00		255.703		2.123		0.147		278.232
	ALPHA=	0.975	TMC=	285.733	TSKT=	9.193	TSG=	9.250
45.00		255.707		2.295		0.159		278.244
	ALPHA=	0.973	TMC=	285.736	TSKT=	9.941	TSG=	10.008
50.00		255.710		2.516		0.175		278.259
	ALPHA=	0.970	TMC=	285.741	TSKT=	10.909	TSG=	10.990
55.00		255.717		2.808		0.196		278.278
	ALPHA=	0.967	TMC=	285.747	TSKT=	12.187	TSG=	12.287
60.00		255.724		3.203		0.225		278.305
	ALPHA=	0.962	TMC=	285.756	TSKT=	13.921	TSG=	14.050
65.00		255.729		3.758		0.266		278.342
	ALPHA=	0.955	TMC=	285.768	TSKT=	16.370	TSG=	16.547
70.00		255.747		4.586		0.329		278.401
	ALPHA=	0.945	TMC=	285.786	TSKT=	20.042	TSG=	20.305
75.00		255.776		5.933		0.435		278.500
	ALPHA=	0.928	TMC=	285.818	TSKT=	26.081	TSG=	26.522
80.00		255.833		8.474		0.648		278.701
	ALPHA=	0.895	TMC=	285.885	TSKT=	37.707	TSG=	38.619
85.00		256.006		14.849		1.291		279.314
	ALPHA=	0.801	TMC=	286.104	TSKT=	68.820	TSG=	71.809

Table 5.6 (Continued)

(b) CLOUD WATER = 1.0, RAIN 0.0

DEGREE		TM		TS		TAOSS.DB		TMG
0.0		255.678		1.540		0.380		277.344
	ALPHA=	0.922	TMC=	279.024	TSKT=	23.083	TSG=	23.216
5.00		255.679		1.545		0.381		277.345
	ALPHA=	0.922	TMC=	279.025	TSKT=	23.167	TSG=	23.301
10.00		255.678		1.562		0.386		277.348
	ALPHA=	0.921	TMC=	279.027	TSKT=	23.422	TSG=	23.559
15.00		255.678		1.590		0.393		277.352
	ALPHA=	0.920	TMC=	279.030	TSKT=	23.857	TSG=	24.000
20.00		255.679		1.630		0.404		277.358
	ALPHA=	0.918	TMC=	279.034	TSKT=	24.490	TSG=	24.639
25.00		255.685		1.685		0.419		277.367
	ALPHA=	0.915	TMC=	279.040	TSKT=	25.346	TSG=	25.505
30.00		255.687		1.755		0.438		277.378
	ALPHA=	0.911	TMC=	279.049	TSKT=	26.461	TSG=	26.633
35.00		255.689		1.846		0.463		277.393
	ALPHA=	0.906	TMC=	279.059	TSKT=	27.889	TSG=	28.070
40.00		255.689		1.959		0.496		277.412
	ALPHA=	0.900	TMC=	279.073	TSKT=	29.705	TSG=	29.919
45.00		255.694		2.103		0.537		277.437
	ALPHA=	0.892	TMC=	279.092	TSKT=	32.018	TSG=	32.265
50.00		255.698		2.287		0.591		277.469
	ALPHA=	0.882	TMC=	279.116	TSKT=	34.992	TSG=	35.283
55.00		255.708		2.522		0.662		277.514
	ALPHA=	0.869	TMC=	279.150	TSKT=	38.877	TSG=	39.232
60.00		255.716		2.832		0.759		277.577
	ALPHA=	0.851	TMC=	279.198	TSKT=	44.078	TSG=	44.527
65.00		255.729		3.249		0.898		277.671
	ALPHA=	0.826	TMC=	279.272	TSKT=	51.291	TSG=	51.887
70.00		255.745		3.831		1.110		277.823
	ALPHA=	0.790	TMC=	279.393	TSKT=	61.822	TSG=	62.663
75.00		255.774		4.678		1.467		278.102
	ALPHA=	0.732	TMC=	279.624	TSKT=	78.418	TSG=	79.716
80.00		255.833		5.946		2.186		278.754
	ALPHA=	0.628	TMC=	280.185	TSKT=	107.994	TSG=	110.262
85.00		256.004		7.330		4.356		281.384
	ALPHA=	0.396	TMC=	282.586	TSKT=	173.683	TSG=	178.183

Table 5.6 (Continued)

(c) CLOUD WATER = 2.0, RAIN 0.0

DEGREE		TM		TS		TADSS.DB		TMG
0.0		255.671		1.448		0.647		277.294
	ALPHA=	0.867	TMC=	278.217	TSKT=	38.157	TSG=	38.372
5.00		255.675		1.453		0.649		277.295
	ALPHA=	0.867	TMC=	278.218	TSKT=	38.292	TSG=	38.508
10.00		255.676		1.467		0.657		277.300
	ALPHA=	0.865	TMC=	278.222	TSKT=	38.700	TSG=	38.922
15.00		255.678		1.492		0.670		277.308
	ALPHA=	0.863	TMC=	278.229	TSKT=	39.398	TSG=	39.626
20.00		255.678		1.527		0.688		277.319
	ALPHA=	0.859	TMC=	278.239	TSKT=	40.410	TSG=	40.649
25.00		255.675		1.574		0.714		277.335
	ALPHA=	0.855	TMC=	278.252	TSKT=	41.775	TSG=	42.029
30.00		255.683		1.635		0.747		277.356
	ALPHA=	0.848	TMC=	278.270	TSKT=	43.550	TSG=	43.824
35.00		255.683		1.712		0.790		277.384
	ALPHA=	0.841	TMC=	278.294	TSKT=	45.815	TSG=	46.116
40.00		255.691		1.808		0.844		277.420
	ALPHA=	0.830	TMC=	278.326	TSKT=	48.584	TSG=	49.019
45.00		255.692		1.928		0.915		277.468
	ALPHA=	0.818	TMC=	278.369	TSKT=	52.317	TSG=	52.700
50.00		255.698		2.078		1.006		277.534
	ALPHA=	0.801	TMC=	278.427	TSKT=	56.955	TSG=	57.401
55.00		255.707		2.266		1.128		277.626
	ALPHA=	0.780	TMC=	278.509	TSKT=	62.958	TSG=	63.492
60.00		255.715		2.504		1.294		277.760
	ALPHA=	0.752	TMC=	278.630	TSKT=	70.894	TSG=	71.555
65.00		255.728		2.809		1.531		277.967
	ALPHA=	0.714	TMC=	278.821	TSKT=	81.714	TSG=	82.562
70.00		255.745		3.200		1.891		278.323
	ALPHA=	0.660	TMC=	279.152	TSKT=	97.119	TSG=	98.260
75.00		255.772		3.688		2.499		279.024
	ALPHA=	0.577	TMC=	279.816	TSKT=	120.459	TSG=	122.089
80.00		255.831		4.172		3.725		280.819
	ALPHA=	0.441	TMC=	281.547	TSKT=	159.314	TSG=	161.716
85.00		256.001		3.619		7.422		288.985
	ALPHA=	0.195	TMC=	289.564	TSKT=	233.696	TSG=	236.660

Table 5.6 (Continued)

(d) CLOUD WATER = 3.0, RAIN 0.0

DEGREE		TM		TS		TAOSS,DB		TMG
0.0		255.679		1.362		0.914		277.381
	ALPHA=	0.816	TMC=	278.007	TSKT=	52.362	TSG=	52.644
5.00		255.669		1.366		0.918		277.383
	ALPHA=	0.815	TMC=	278.010	TSKT=	52.541	TSG=	52.825
10.00		255.683		1.378		0.928		277.391
	ALPHA=	0.813	TMC=	278.017	TSKT=	53.085	TSG=	53.375
15.00		255.679		1.400		0.946		277.404
	ALPHA=	0.810	TMC=	278.029	TSKT=	54.013	TSG=	54.311
20.00		255.678		1.430		0.973		277.423
	ALPHA=	0.805	TMC=	278.047	TSKT=	55.356	TSG=	55.668
25.00		255.679		1.471		1.009		277.450
	ALPHA=	0.799	TMC=	278.071	TSKT=	57.165	TSG=	57.496
30.00		255.685		1.523		1.055		277.485
	ALPHA=	0.790	TMC=	278.104	TSKT=	59.512	TSG=	59.866
35.00		255.683		1.588		1.116		277.532
	ALPHA=	0.780	TMC=	278.148	TSKT=	62.496	TSG=	62.882
40.00		255.694		1.669		1.193		277.595
	ALPHA=	0.766	TMC=	278.207	TSKT=	66.258	TSG=	66.687
45.00		255.691		1.767		1.293		277.679
	ALPHA=	0.750	TMC=	278.286	TSKT=	71.000	TSG=	71.483
50.00		255.696		1.888		1.422		277.795
	ALPHA=	0.728	TMC=	278.395	TSKT=	77.009	TSG=	77.566
55.00		255.701		2.035		1.594		277.959
	ALPHA=	0.701	TMC=	278.552	TSKT=	84.717	TSG=	85.373
60.00		255.713		2.214		1.828		278.204
	ALPHA=	0.665	TMC=	278.786	TSKT=	94.788	TSG=	95.580
65.00		255.727		2.428		2.163		278.593
	ALPHA=	0.617	TMC=	279.161	TSKT=	108.294	TSG=	109.279
70.00		255.740		2.673		2.672		279.274
	ALPHA=	0.551	TMC=	279.822	TSKT=	127.078	TSG=	128.340
75.00		255.769		2.908		3.532		280.660
	ALPHA=	0.455	TMC=	281.179	TSKT=	154.547	TSG=	156.201
80.00		255.828		2.928		5.264		284.321
	ALPHA=	0.309	TMC=	284.792	TSKT=	197.615	TSG=	199.707
85.00		255.729		1.785		10.487		301.401
	ALPHA=	0.097	TMC=	301.754	TSKT=	272.801	TSG=	274.459

Table 5.6 (Continued)

(e) CLOUD WATER = 4.0, RAIN 0.0

TEGREE		TM		TS		TAOSS.DB		TMG
0.0		255.677		1.280		1.181		277.541
	ALPHA=	0.767	TMC=	278.011	TSKT=	65.755	TSG=	66.092
5.00		255.678		1.284		1.186		277.545
	ALPHA=	0.766	TMC=	278.014	TSKT=	65.973	TSG=	66.312
10.00		255.678		1.295		1.199		277.556
	ALPHA=	0.764	TMC=	278.025	TSKT=	66.636	TSG=	66.981
15.00		255.679		1.313		1.223		277.576
	ALPHA=	0.760	TMC=	278.044	TSKT=	67.765	TSG=	68.119
20.00		255.677		1.339		1.257		277.606
	ALPHA=	0.754	TMC=	278.073	TSKT=	69.397	TSG=	69.767
25.00		255.682		1.374		1.303		277.647
	ALPHA=	0.746	TMC=	278.112	TSKT=	71.592	TSG=	71.981
30.00		255.684		1.418		1.364		277.702
	ALPHA=	0.736	TMC=	278.164	TSKT=	74.430	TSG=	74.847
35.00		255.687		1.473		1.442		277.775
	ALPHA=	0.723	TMC=	278.235	TSKT=	78.029	TSG=	78.481
40.00		255.688		1.540		1.542		277.873
	ALPHA=	0.707	TMC=	278.329	TSKT=	82.548	TSG=	83.045
45.00		255.692		1.620		1.670		278.006
	ALPHA=	0.687	TMC=	278.458	TSKT=	88.213	TSG=	88.769
50.00		255.700		1.716		1.838		278.190
	ALPHA=	0.662	TMC=	278.636	TSKT=	95.345	TSG=	95.977
55.00		255.705		1.828		2.059		278.453
	ALPHA=	0.630	TMC=	278.892	TSKT=	104.415	TSG=	105.147
60.00		255.715		1.957		2.362		278.850
	ALPHA=	0.588	TMC=	279.280	TSKT=	116.129	TSG=	116.994
65.00		255.723		2.099		2.795		279.487
	ALPHA=	0.534	TMC=	279.905	TSKT=	131.598	TSG=	132.640
70.00		255.741		2.233		3.454		280.616
	ALPHA=	0.460	TMC=	281.019	TSKT=	152.651	TSG=	153.924
75.00		255.770		2.292		4.564		282.945
	ALPHA=	0.359	TMC=	283.325	TSKT=	182.476	TSG=	184.017
80.00		255.825		2.054		6.802		289.172
	ALPHA=	0.217	TMC=	289.514	TSKT=	227.114	TSG=	228.787
85.00		255.428		0.880		13.553		318.194
	ALPHA=	0.048	TMC=	318.421	TSKT=	303.283	TSG=	304.152

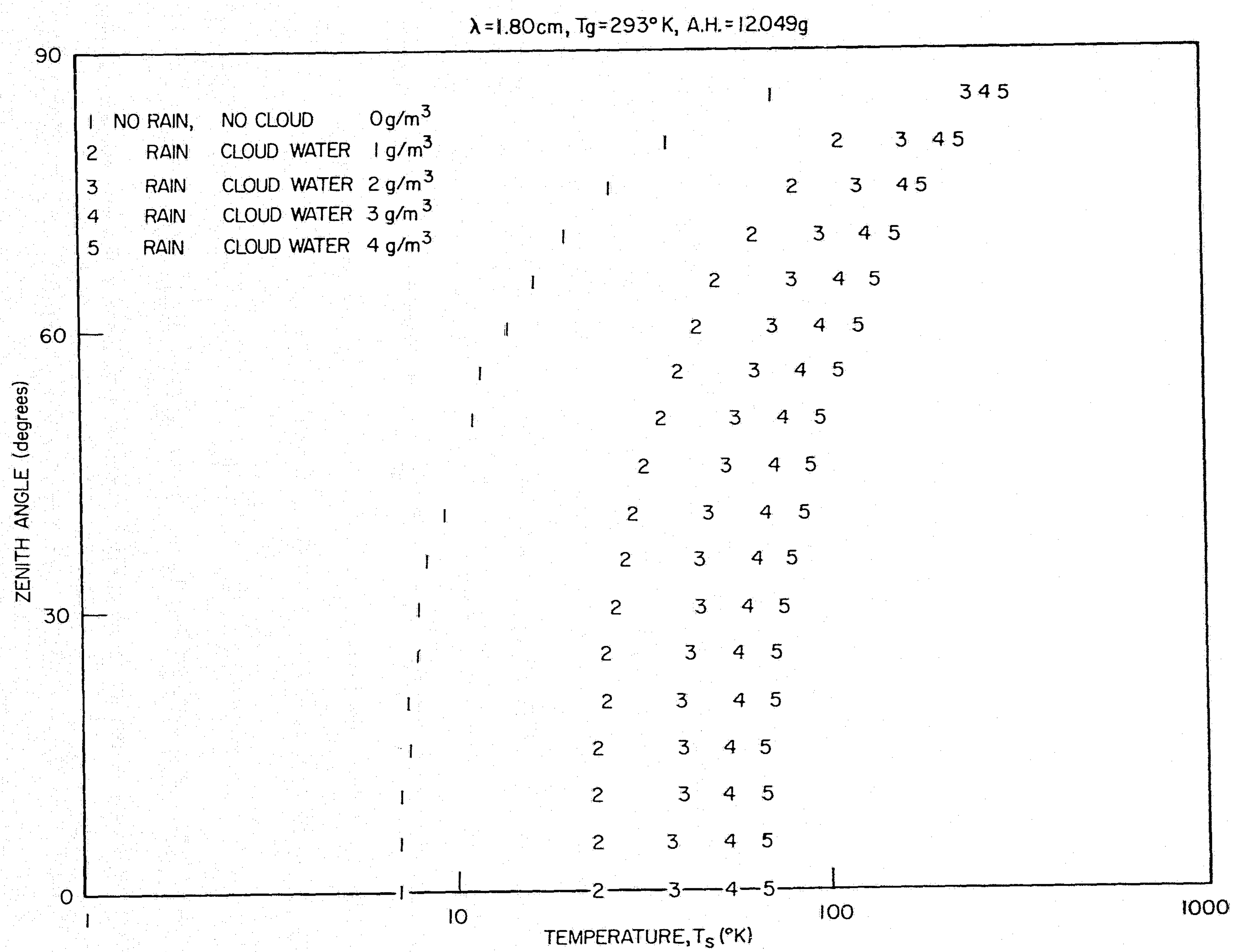

Figure 5.8. Sky temperature versus zenith angle for the 16 GHz radiometer.

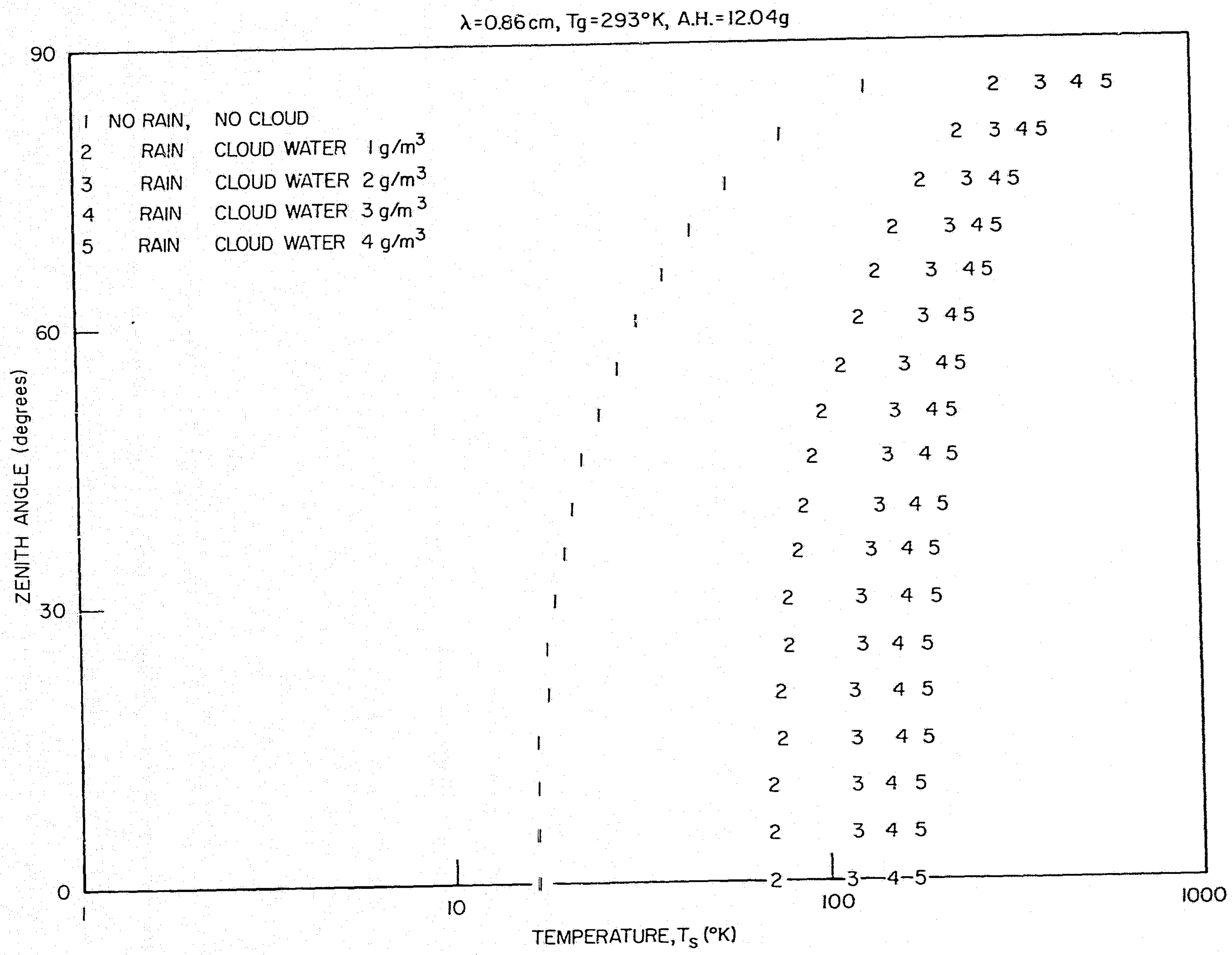

Figure 5.9. Sky temperature versus zenith angle for the 35 GHz radiometer.

Table 5.7—Calculated Data Used for Figure 5.9 (λ = 0.86 (35 GHz) GT = 293°K, R. H. = 70%)

(a) CLOUD WATER = 0.0, RAIN 0.0

DEGREE		TM		TS		TAOSS,DB		TMG
0.0		255.232		3.861		0.268		278.075
	ALPHA=	0.955	TMC=	285.819	TSKT=	16.437	TSG=	16.617
5.00		255.232		3.875		0.269		278.075
	ALPHA=	0.955	TMC=	285.819	TSKT=	16.497	TSG=	16.679
10.00		255.234		3.918		0.272		278.079
	ALPHA=	0.955	TMC=	285.820	TSKT=	16.680	TSG=	16.866
15.00		255.235		3.990		0.277		278.084
	ALPHA=	0.954	TMC=	285.821	TSKT=	16.993	TSG=	17.185
20.00		255.238		4.095		0.285		278.091
	ALPHA=	0.953	TMC=	285.823	TSKT=	17.447	TSG=	17.650
25.00		255.239		4.237		0.295		278.101
	ALPHA=	0.951	TMC=	285.827	TSKT=	18.062	TSG=	18.279
30.00		255.243		4.422		0.309		278.114
	ALPHA=	0.949	TMC=	285.831	TSKT=	18.864	TSG=	19.100
35.00		255.247		4.659		0.327		278.131
	ALPHA=	0.946	TMC=	285.836	TSKT=	19.891	TSG=	20.154
40.00		255.254		4.959		0.349		278.153
	ALPHA=	0.942	TMC=	285.843	TSKT=	21.200	TSG=	21.497
45.00		255.262		5.342		0.378		278.181
	ALPHA=	0.938	TMC=	285.851	TSKT=	22.869	TSG=	23.215
50.00		255.272		5.832		0.416		278.217
	ALPHA=	0.931	TMC=	285.862	TSKT=	25.019	TSG=	25.432
55.00		255.287		6.471		0.467		278.266
	ALPHA=	0.924	TMC=	285.878	TSKT=	27.835	TSG=	28.344
60.00		255.307		7.322		0.535		278.332
	ALPHA=	0.913	TMC=	285.899	TSKT=	31.616	TSG=	32.271
65.00		255.335		8.495		0.633		278.427
	ALPHA=	0.898	TMC=	285.929	TSKT=	36.886	TSG=	37.774
70.00		255.376		10.190		0.782		278.571
	ALPHA=	0.875	TMC=	285.977	TSKT=	44.631	TSG=	45.926
75.00		255.446		12.808		1.034		278.816
	ALPHA=	0.838	TMC=	286.062	TSKT=	56.970	TSG=	59.069
80.00		255.588		17.258		1.541		279.316
	ALPHA=	0.769	TMC=	286.246	TSKT=	79.410	TSG=	83.436
85.00		256.024		25.376		3.070		280.876
	ALPHA=	0.592	TMC=	286.917	TSKT=	131.965	TSG=	142.368

Table 5.7 (Continued)

(b) CLOUD WATER = 1.0, RAIN 0.0

DEGREE		TM		TS		TAOSS,DB		TMG
0.0		255.232		3.039		1.307		277.771
	ALPHA=	0.752	TMC=	278.852	TSKT=	71.408	TSG=	72.202
5.00		255.228		3.047		1.312		277.774
	ALPHA=	0.751	TMC=	278.856	TSKT=	71.641	TSG=	72.439
10.00		255.229		3.072		1.327		277.787
	ALPHA=	0.749	TMC=	278.867	TSKT=	72.346	TSG=	73.159
15.00		255.235		3.114		1.353		277.809
	ALPHA=	0.745	TMC=	278.886	TSKT=	73.547	TSG=	74.364
20.00		255.237		3.174		1.391		277.841
	ALPHA=	0.738	TMC=	278.915	TSKT=	75.282	TSG=	76.155
25.00		255.241		3.253		1.442		277.885
	ALPHA=	0.730	TMC=	278.955	TSKT=	77.612	TSG=	78.533
30.00		255.242		3.354		1.510		277.944
	ALPHA=	0.720	TMC=	279.008	TSKT=	80.622	TSG=	81.607
35.00		255.249		3.478		1.596		278.023
	ALPHA=	0.706	TMC=	279.078	TSKT=	84.429	TSG=	85.497
40.00		255.255		3.628		1.707		278.126
	ALPHA=	0.689	TMC=	279.173	TSKT=	89.198	TSG=	90.374
45.00		255.262		3.807		1.849		278.266
	ALPHA=	0.668	TMC=	279.300	TSKT=	95.158	TSG=	96.472
50.00		255.274		4.018		2.034		278.456
	ALPHA=	0.642	TMC=	279.475	TSKT=	102.632	TSG=	104.124
55.00		255.288		4.262		2.279		278.726
	ALPHA=	0.609	TMC=	279.725	TSKT=	112.086	TSG=	113.812
60.00		255.307		4.536		2.615		279.124
	ALPHA=	0.566	TMC=	280.097	TSKT=	124.217	TSG=	126.249
65.00		255.334		4.821		3.093		279.751
	ALPHA=	0.510	TMC=	280.690	TSKT=	140.095	TSG=	142.524
70.00		255.375		5.060		3.822		280.835
	ALPHA=	0.435	TMC=	281.727	TSKT=	161.433	TSG=	164.363
75.00		255.447		5.078		5.051		282.997
	ALPHA=	0.333	TMC=	283.817	TSKT=	191.090	TSG=	194.550
80.00		255.586		4.347		7.528		288.484
	ALPHA=	0.194	TMC=	289.178	TSKT=	233.952	TSG=	237.518
85.00		255.779		1.626		14.999		310.894
	ALPHA=	0.038	TMC=	311.258	TSKT=	299.470	TSG=	301.061

Table 5.7 (Continued)

(c) CLOUD WATER = 2.0, RAIN 0.0

DEGREE		TM		TS		TAOSS.DB		TMG
0.0		255.230		2.392		2.347		278.802
	ALPHA=	0.592	TMC=	279.343	TSKT=	115.364	TSG=	116.398
5.00		255.226		2.396		2.356		278.813
	ALPHA=	0.591	TMC=	279.354	TSKT=	115.699	TSG=	116.738
10.00		255.229		2.409		2.383		278.850
	ALPHA=	0.587	TMC=	279.390	TSKT=	116.713	TSG=	117.767
15.00		255.232		2.430		2.430		278.913
	ALPHA=	0.581	TMC=	279.451	TSKT=	118.435	TSG=	119.513
20.00		255.235		2.460		2.498		279.006
	ALPHA=	0.573	TMC=	279.542	TSKT=	120.912	TSG=	122.024
25.00		255.231		2.498		2.590		279.136
	ALPHA=	0.561	TMC=	279.669	TSKT=	124.214	TSG=	125.373
30.00		255.236		2.544		2.710		279.312
	ALPHA=	0.546	TMC=	279.840	TSKT=	128.443	TSG=	129.660
35.00		255.245		2.596		2.865		279.547
	ALPHA=	0.527	TMC=	280.069	TSKT=	133.732	TSG=	135.023
40.00		255.253		2.654		3.064		279.862
	ALPHA=	0.505	TMC=	280.378	TSKT=	140.263	TSG=	141.644
45.00		255.261		2.714		3.319		280.291
	ALPHA=	0.477	TMC=	280.799	TSKT=	148.278	TSG=	149.766
50.00		255.271		2.769		3.651		280.889
	ALPHA=	0.442	TMC=	281.387	TSKT=	158.104	TSG=	159.716
55.00		255.286		2.808		4.092		281.751
	ALPHA=	0.401	TMC=	282.237	TSKT=	170.180	TSG=	171.932
60.00		255.305		2.810		4.694		283.053
	ALPHA=	0.351	TMC=	283.523	TSKT=	185.114	TSG=	187.009
65.00		255.334		2.736		5.553		285.151
	ALPHA=	0.289	TMC=	285.600	TSKT=	203.754	TSG=	205.768
70.00		255.370		2.513		6.862		288.862
	ALPHA=	0.216	TMC=	289.283	TSKT=	227.334	TSG=	229.368
75.00		255.189		2.012		9.068		296.404
	ALPHA=	0.132	TMC=	296.778	TSKT=	257.869	TSG=	259.669
80.00		255.217		1.094		13.516		315.598
	ALPHA=	0.049	TMC=	315.870	TSKT=	300.480	TSG=	301.552
85.00		251.550		0.103		26.929		388.033
	ALPHA=	0.002	TMC=	388.089	TSKT=	387.140	TSG=	387.246

Table 5.7 (Continued)

(d) CLOUD WATER = 3.0, RAIN 0.0

DEGREE		TM		TS		TAOSS.DB		TMG
0.0		255.228		1.883		3.387		280.533
	ALPHA=	0.466	TMC=	280.882	TSKT=	150.838	TSG=	151.911
5.00		255.225		1.884		3.400		280.557
	ALPHA=	0.465	TMC=	280.906	TSKT=	151.231	TSG=	152.307
10.00		255.225		1.889		3.439		280.632
	ALPHA=	0.461	TMC=	280.981	TSKT=	152.417	TSG=	153.504
15.00		255.232		1.897		3.506		280.762
	ALPHA=	0.454	TMC=	281.110	TSKT=	154.424	TSG=	155.529
20.00		255.234		1.907		3.604		280.955
	ALPHA=	0.444	TMC=	281.301	TSKT=	157.299	TSG=	158.428
25.00		255.232		1.918		3.737		281.224
	ALPHA=	0.431	TMC=	281.567	TSKT=	161.111	TSG=	162.273
30.00		255.237		1.929		3.911		281.589
	ALPHA=	0.414	TMC=	281.928	TSKT=	165.955	TSG=	167.155
35.00		255.240		1.938		4.134		282.078
	ALPHA=	0.394	TMC=	282.414	TSKT=	171.957	TSG=	173.203
40.00		255.244		1.942		4.421		282.737
	ALPHA=	0.369	TMC=	283.068	TSKT=	179.282	TSG=	180.577
45.00		255.255		1.934		4.790		283.638
	ALPHA=	0.340	TMC=	283.964	TSKT=	188.142	TSG=	189.490
50.00		255.267		1.908		5.269		284.900
	ALPHA=	0.305	TMC=	285.219	TSKT=	198.817	TSG=	200.213
55.00		255.280		1.850		5.905		286.726
	ALPHA=	0.264	TMC=	287.036	TSKT=	211.674	TSG=	213.103
60.00		255.300		1.741		6.773		289.495
	ALPHA=	0.217	TMC=	289.792	TSKT=	227.211	TSG=	228.639
65.00		255.317		1.553		8.014		293.970
	ALPHA=	0.164	TMC=	294.252	TSKT=	246.168	TSG=	247.525
70.00		255.026		1.246		9.902		301.883
	ALPHA=	0.107	TMC=	302.139	TSKT=	269.844	TSG=	271.006
75.00		254.989		0.797		13.085		317.847
	ALPHA=	0.052	TMC=	318.054	TSKT=	301.437	TSG=	302.226
80.00		254.233		0.274		19.503		357.367
	ALPHA=	0.012	TMC=	357.479	TSKT=	353.076	TSG=	353.360
85.00		196.115		0.005		38.858		492.257
	ALPHA=	0.000	TMC=	492.264	TSKT=	492.187	TSG=	492.193

Table 5.7 (Continued)

(e) CLOUD WATER = 4.0, RAIN 0.0

DEGREE		TM		TS		TADSS.DB		TMG
0.0		255.214		1.482		4.426		282.919
	ALPHA=	0.367	TMC=	283.173	TSKT=	179.811	TSG=	180.820
5.00		255.222		1.482		4.443		282.961
	ALPHA=	0.366	TMC=	283.215	TSKT=	180.233	TSG=	181.244
10.00		255.227		1.481		4.495		283.089
	ALPHA=	0.361	TMC=	283.342	TSKT=	181.505	TSG=	182.522
15.00		255.232		1.480		4.583		283.312
	ALPHA=	0.354	TMC=	283.564	TSKT=	183.655	TSG=	184.681
20.00		255.231		1.478		4.710		283.642
	ALPHA=	0.344	TMC=	283.892	TSKT=	186.723	TSG=	187.763
25.00		255.228		1.473		4.884		284.102
	ALPHA=	0.331	TMC=	284.351	TSKT=	190.773	TSG=	191.829
30.00		255.234		1.463		5.111		284.726
	ALPHA=	0.314	TMC=	284.972	TSKT=	195.889	TSG=	196.963
35.00		255.238		1.447		5.404		285.564
	ALPHA=	0.294	TMC=	285.808	TSKT=	202.185	TSG=	203.276
40.00		255.241		1.421		5.778		286.697
	ALPHA=	0.270	TMC=	286.936	TSKT=	209.804	TSG=	210.909
45.00		255.251		1.379		6.260		288.246
	ALPHA=	0.242	TMC=	288.481	TSKT=	218.936	TSG=	220.048
50.00		255.259		1.314		6.886		290.417
	ALPHA=	0.210	TMC=	290.646	TSKT=	229.831	TSG=	230.933
55.00		255.277		1.218		7.717		293.560
	ALPHA=	0.174	TMC=	293.781	TSKT=	242.836	TSG=	243.903
60.00		254.877		1.077		8.853		298.321
	ALPHA=	0.135	TMC=	298.533	TSKT=	258.483	TSG=	259.470
65.00		254.815		0.879		10.474		306.001
	ALPHA=	0.093	TMC=	306.196	TSKT=	277.720	TSG=	278.564
70.00		254.755		0.618		12.942		319.501
	ALPHA=	0.053	TMC=	319.667	TSKT=	302.653	TSG=	303.272
75.00		253.867		0.335		17.102		346.349
	ALPHA=	0.021	TMC=	346.466	TSKT=	339.272	TSG=	339.599
80.00		249.605		0.068		25.491		410.602
	ALPHA=	0.003	TMC=	410.646	TSKT=	409.369	TSG=	409.442
85.00		0.0		0.0		50.787		609.355
	ALPHA=	0.000	TMC=	609.356	TSKT=	609.350	TSG=	609.350

The total loss is as follows:

$$\beta_{at} + \beta_{c\ell} + \beta_r = \beta \text{ (in dB)}, \tag{5.11}$$

where

β_{at} = atmospheric gaseous loss,

$\beta_{c\ell}$ = loss due to water cloud

β_r = loss due to rain.

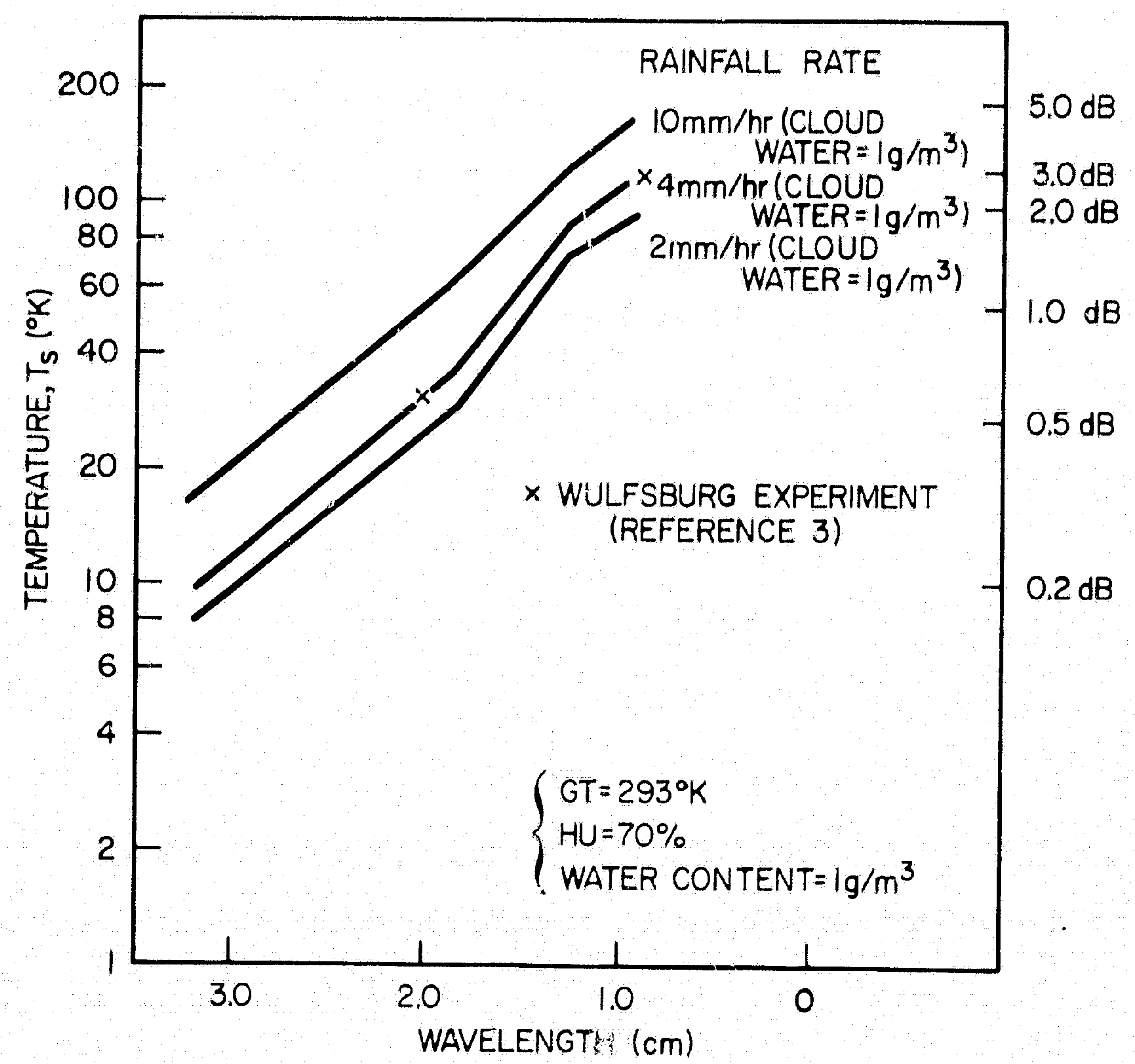

Figure 5.10. Temperature increase due to rain (vertical).

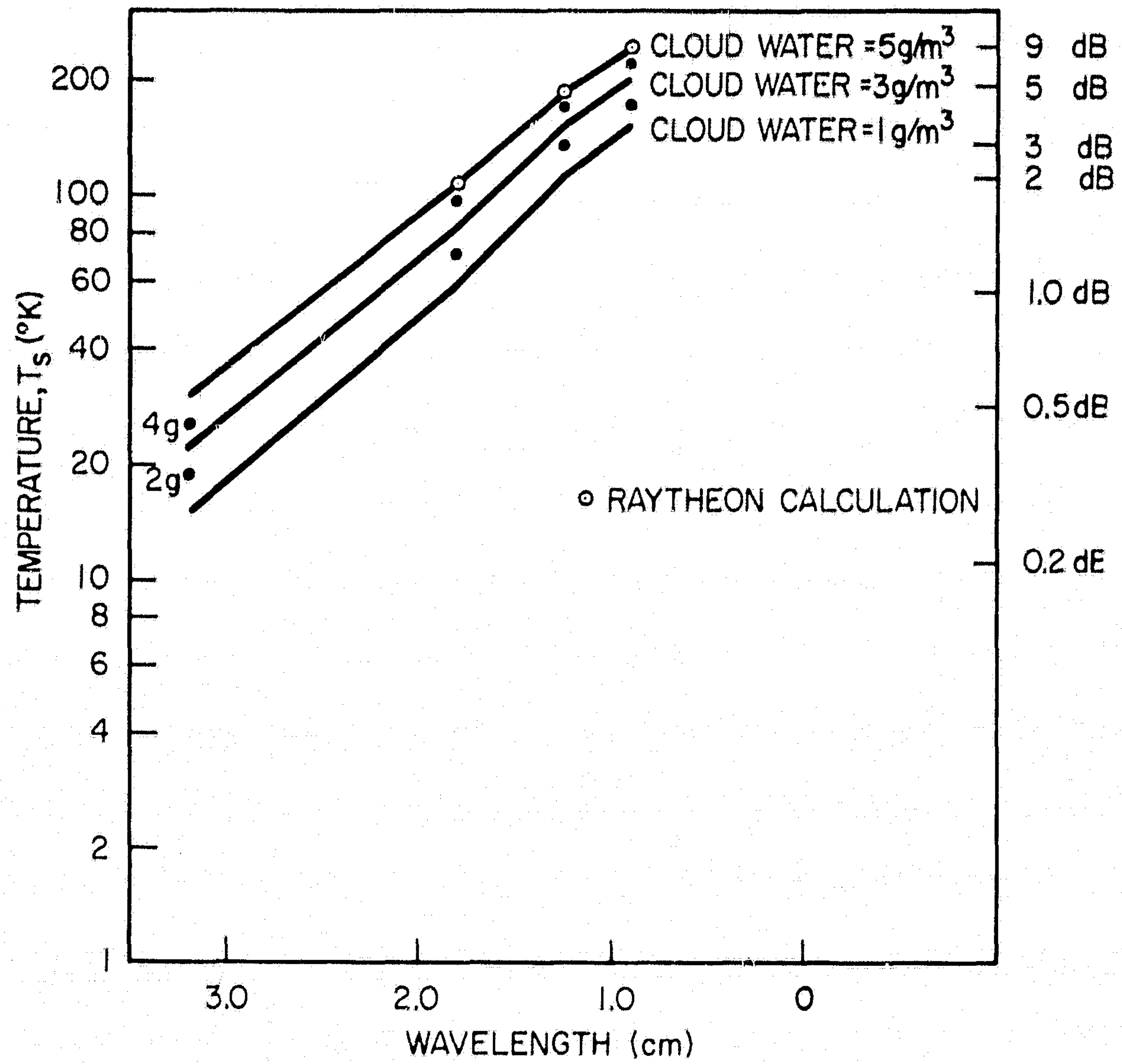

Figure 5.11. Temperature variations (vertical) due to water content of cloud when it rains at the rate of 10 mm/hr.

By changing β into α (fractional transmission coefficient), the temperature calculation was done in the same way as in Section 5.4 (equation (5.10). In Figure 5.10, the temperature increase due to rain and cloud is shown, assuming the cloud water content at $1g/m^3$. Figure 5.11 shows the temperature change due to the water content of the cloud during rains at 10 mm/hr: The change is 155° - 235°K at 35 GHz, and 50°-90°K at 16 GHz, during rainfall at that rate.

6. CONCLUSIONS

The average difference values between the expected and the measured true temperature were 35°K for the 16 GHz radiometer and 24°K for the 35 GHz radiometer. The differences include antenna and feeder losses and the temperature increase due to the radiometer sidelobes hitting surrounding trees.

Taking the surrounding environment into consideration, the estimation of sky temperature increase due to sidelobes was carried out, and values of 4.5°K at 16 GHz and 12°K at 35 GHz were obtained for sidelobe effects.

The correlation between one-point rainfall rate near the radiometers and the measured temperature increase due to rain at a 45° elevation angle was not good during severe summer thunderstorms, but much better for rather light rain (less than 10 mm/hr).

Statistics on the cloud scintillation show that the scintillation number 1 occurred most frequently. The scintillation number reached 10 at its maximum. Computation for the expected sky temperature shows that, under various ground conditions, sky temperature change is very small (3 to 5.5°K) at 15 GHz, but larger temperature changes (8°-18°K) were found at 35 GHz by the method of Shulkin (Reference 1). Data computed by the method of Bean and Dutton (Reference 2) are in good agreement with those calculated by Shulkin's method for the high water vapor content.

Concerning the temperature increase due to rain or cloud, the water content of cloud has an important effect upon the radiometer temperature, reaching above the frequency 30 GHz (see Figure 5.7).

7. ACKNOWLEDGEMENTS

This work was done during the author's stay at GSFC for about a year (Nov. 1968 - Jan. 1970) with the support of all the members of the Extra High Frequency Technology Section. I especially gratefully acknowledge Mr. William O. Binkley, the Section head, for the opportunity to perform the radiometer experiment as an exchange visitor; and Mr. J. Larry King, who engineered both radiometers and who always aided the experiment and gave valuable suggestions. Also I wish to express my heartfelt thanks to Mr. E. Hirschmann, who always helped me in the experiment and gave generously of his time in deep discussion on this paper; and to Dr. E. Mondre who also contributed extensive discussions and suggestions, expecially for the computation of sky temperatures. Finally I am much obliged to Mr. James L. Baker, the ATS Project Office, Ground Support Manager, for his great assistance in the negotiation of my visit to NASA-GSFC.

8. REFERENCES

1. Shulkin, M., "Determination of Microwave Atmospheric Absorption Using Extraterrestrial Sources," Naval Research Laboratory Report 3843, October 1951.

2. Bean, B. R., and Dutton, E. J., "Radio Meteorology," National Bureau of Standards Monograph 92, March 1966.

3. Altshuler, E. E., Falconne, Jr., V. J., and Wulfsburg, K. N., "Atmospheric Effects on the Propagation at Millimeter Wavelengths." I.E.E.E. Spectrum, Vo. 5, pp. 83-90, July 1968.

4. Wulfsburg, K. N., "Apparent Sky Temperature Measurements at Millimeter Wave Frequencies," Physical Sciences Research Papers No. 38, Air Force Cambridge Research Laboratories, July 1964.

5. Snider, J. B., "Proposed Program for the Study of Atmospheric Attenuation of Satellite Signals," Environmental Science Services Administration Technical Report RL62-WPL1, January 1968.

6. "Final Report for Millimeter Communication Propagation Program" extension. 28 May 1966 - 27 Feb. 1967) Volume 1, Sections 1 through 3. Prepared by Raytheon Company, Space and Information Systems Division. Contract No. NAS 5-9525.

7. Mason, B. J., "The Physics of Clouds," Oxford: Clarendon Press, 1957.

8. Van Vleck, J. H. and Weisskopf, V. F., "On the Shape of Collision-Broadened Lines." Rev. Mod. Phys. Vol. 17, Nos. 2 and 3, 227-236, April to July 1945.

9. Van Vleck, J. H., "The Absorption of Microwaves by Oxygen, Phy. Rev. Vol. 71, No. 7, 413-424, April 1947.

10. Van Vleck, J. H., "The Absorption of Microwaves by Uncondensed Water Vapor." Phy. Rev. Vol. 71, No. 7, 425-433, April 1947.

11. Tompson III, W. I., and Haroules, G. G., "A Review of Radiometric Measurements of Atmospheric Attenuation at Wavelengths from 75 cm to 2 mm." NASA TN D-5087, Electronics Research Center, Cambridge, Mass, April 1969.

12. Gunn, K. L. S., and East, T. W. R., "The Microwave Properties of Precipitation Particles." Quat. J. Roy. Met. Soc. Vol 80, 522-545, 1954.

APPENDIX A

Calibration Methods and Their Problems

Two cold loads were used for the linearity check on the recorder; they were:

(a) dry ice + alcohol, -75°C (198°K),

(b) ice cubes + water, 0°C (273°K).

These points have been shown also in the Figure A1. This figure indicates a reasonable linearity of both radiometers.

Calibrations of both radiometers were accomplished by using waveguide switches (WGSW). Besides the difficulties associated with waveguide switching, some calibration difficulties in cold load occurred due to a buildup of dewdrops inside the waveguide between the cold load and the WGSW.

During the cold load calibration, the waveguide was evacuated or filled with high pressure helium gas to avoid an accumulation of water drops, which caused temperature instability.

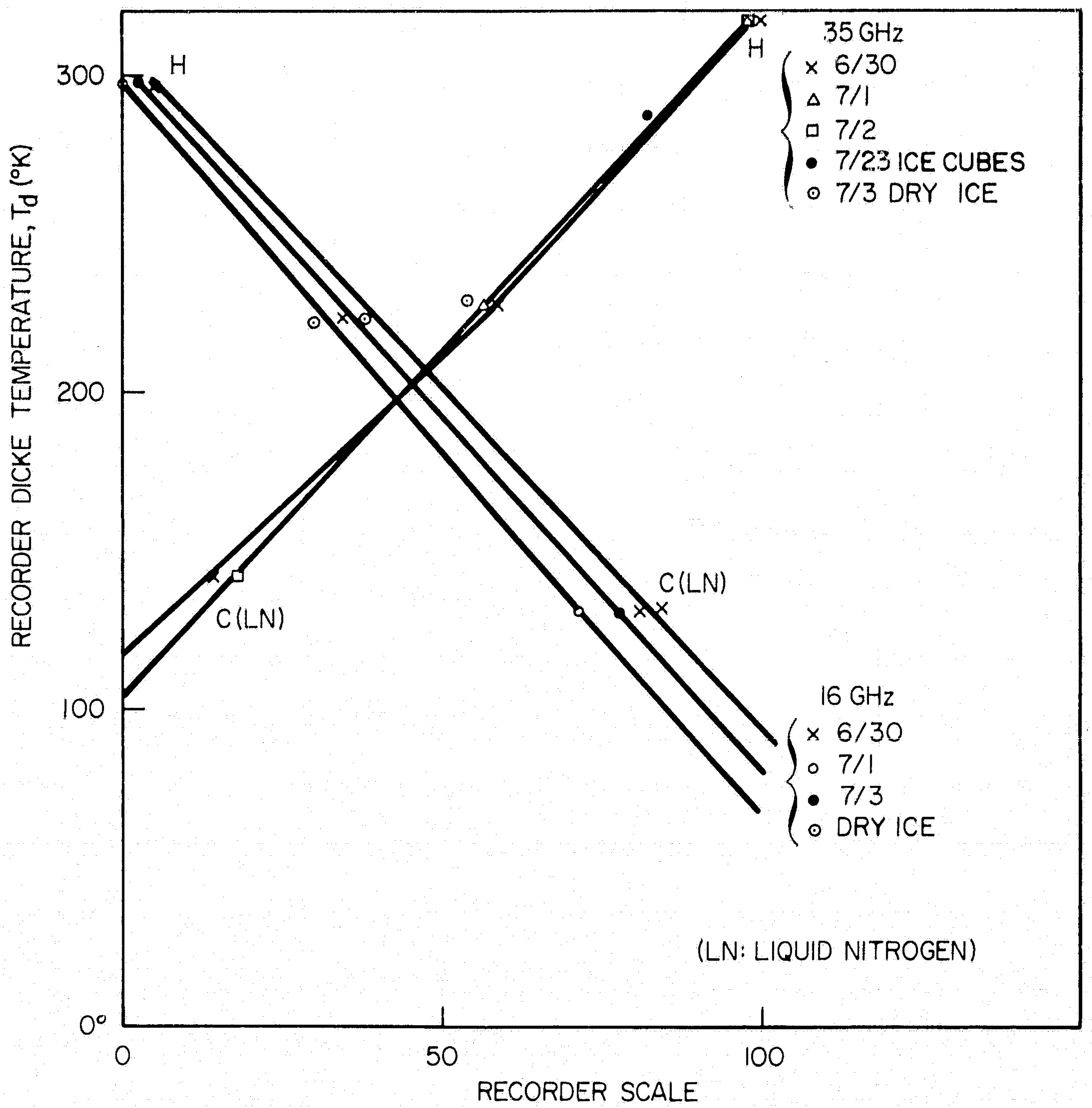

Figure A.1. Radiometer calibrations (July 2).

APPENDIX B

Temperature Drift Problems

When long time changes of sky temperature (say, hourly or daily) are considered, temperature drift must be taken into account. This drift is mainly caused by the system instability.

In Figures B1 through B3 are shown examples of the hourly changes in the temperature indications of both radiometers. In these examples, no typical drift can be found except during the calibration time.

Drift or unnatural change in the temperature can be found, however, in the following circumstances:

(i) Mainly after changing the zero point and scale in the recorder amplifiers.

(ii) After removing the cover from the radiometer package box (this should be avoided after obtaining a uniform temperature in the package).

(iii) After changing the klystron voltage and current working conditions. This change of the klystron (local oscillator) has a large and long-lasting effect upon the mixer before it becomes stable again.

(iv) When working with waveguide switches.

Mixer currents, which have a long time drift due to the change of klystron condition, dc amplifier level, and zero point of the recorders, should be separately recorded for later reference to better understand drift problems in the radiometric data.

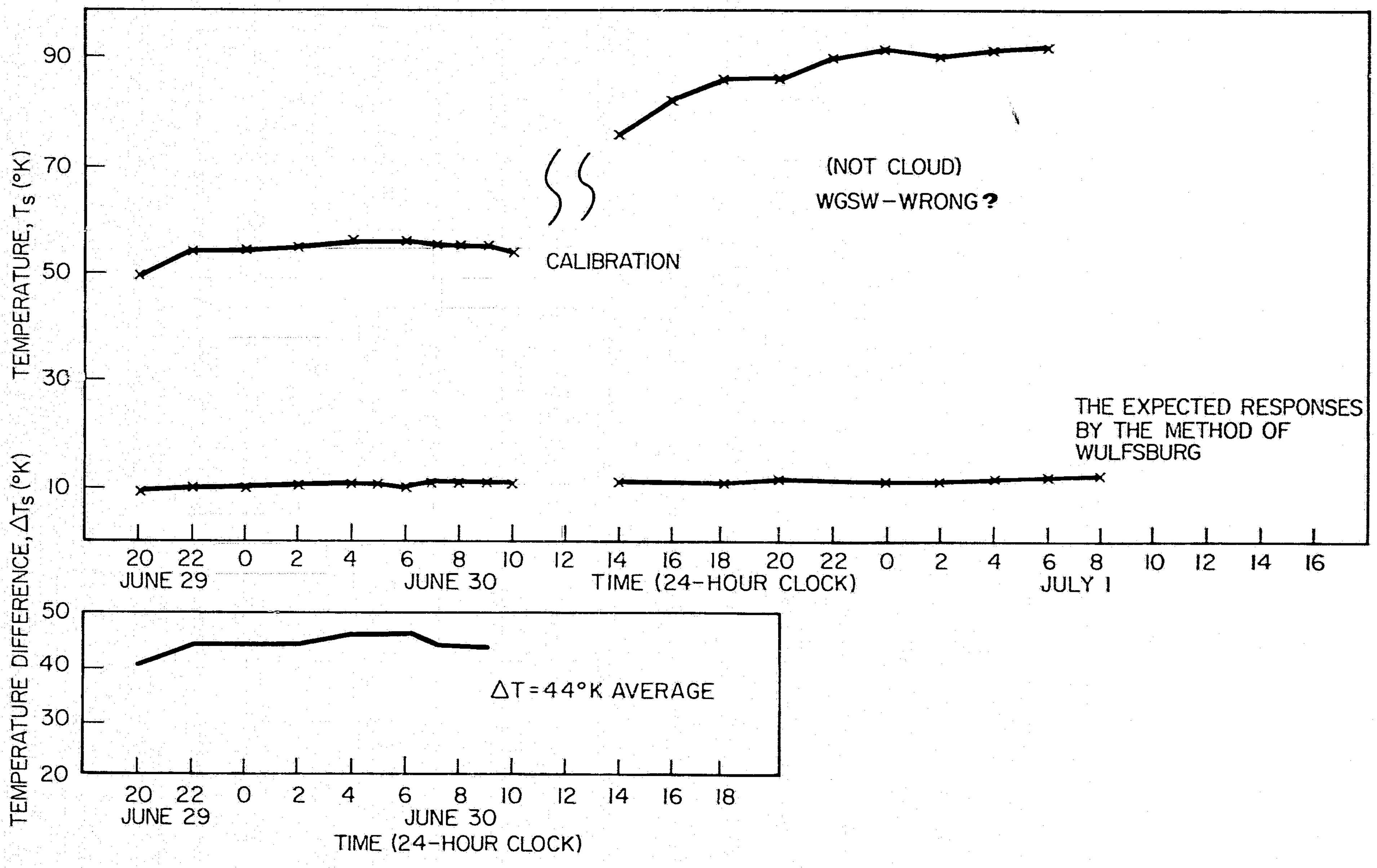

Figure B.1. Two-hourly change for 16 GHz radiometers.

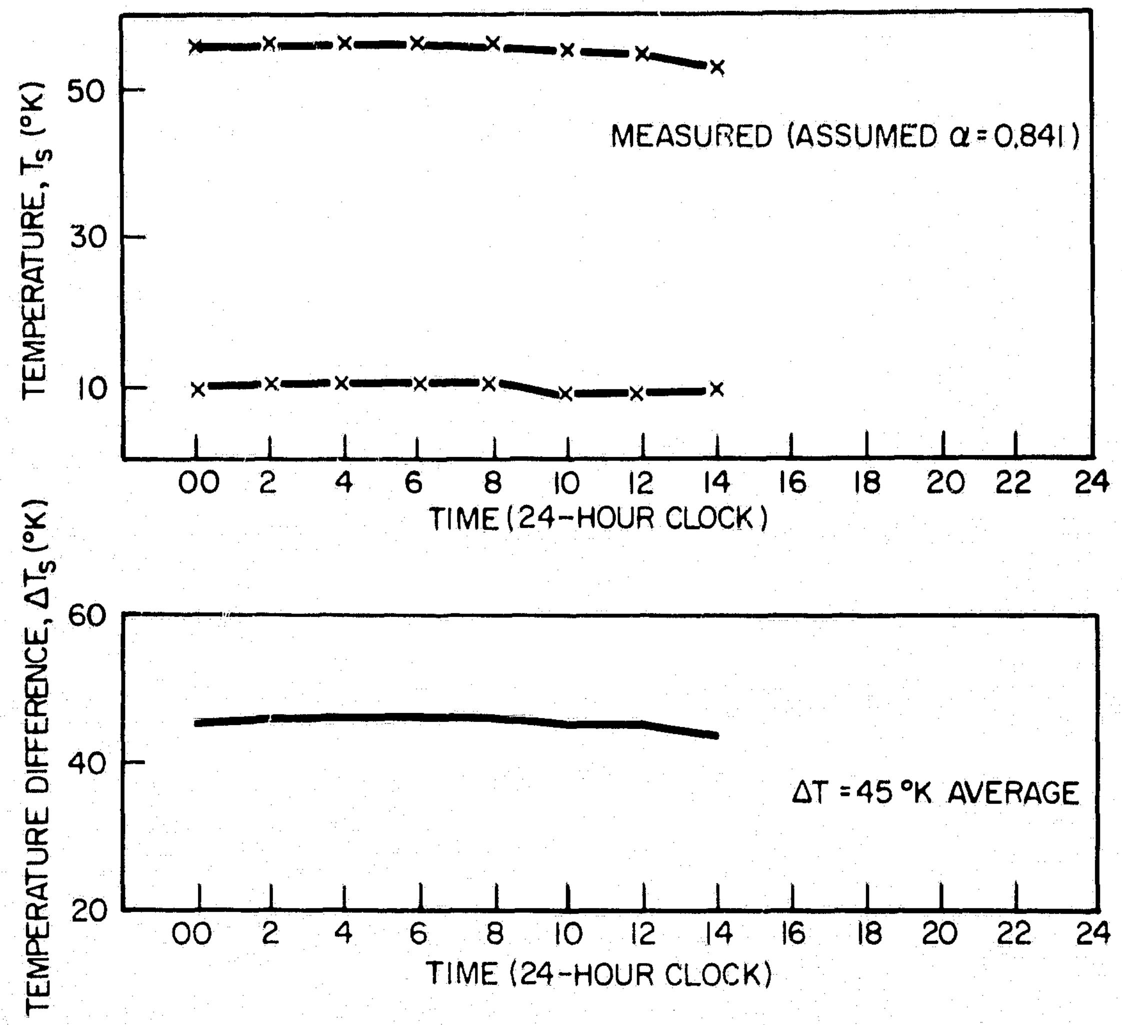

Figure B.2. Two-hourly change for 16 GHz radiometers on June 29.

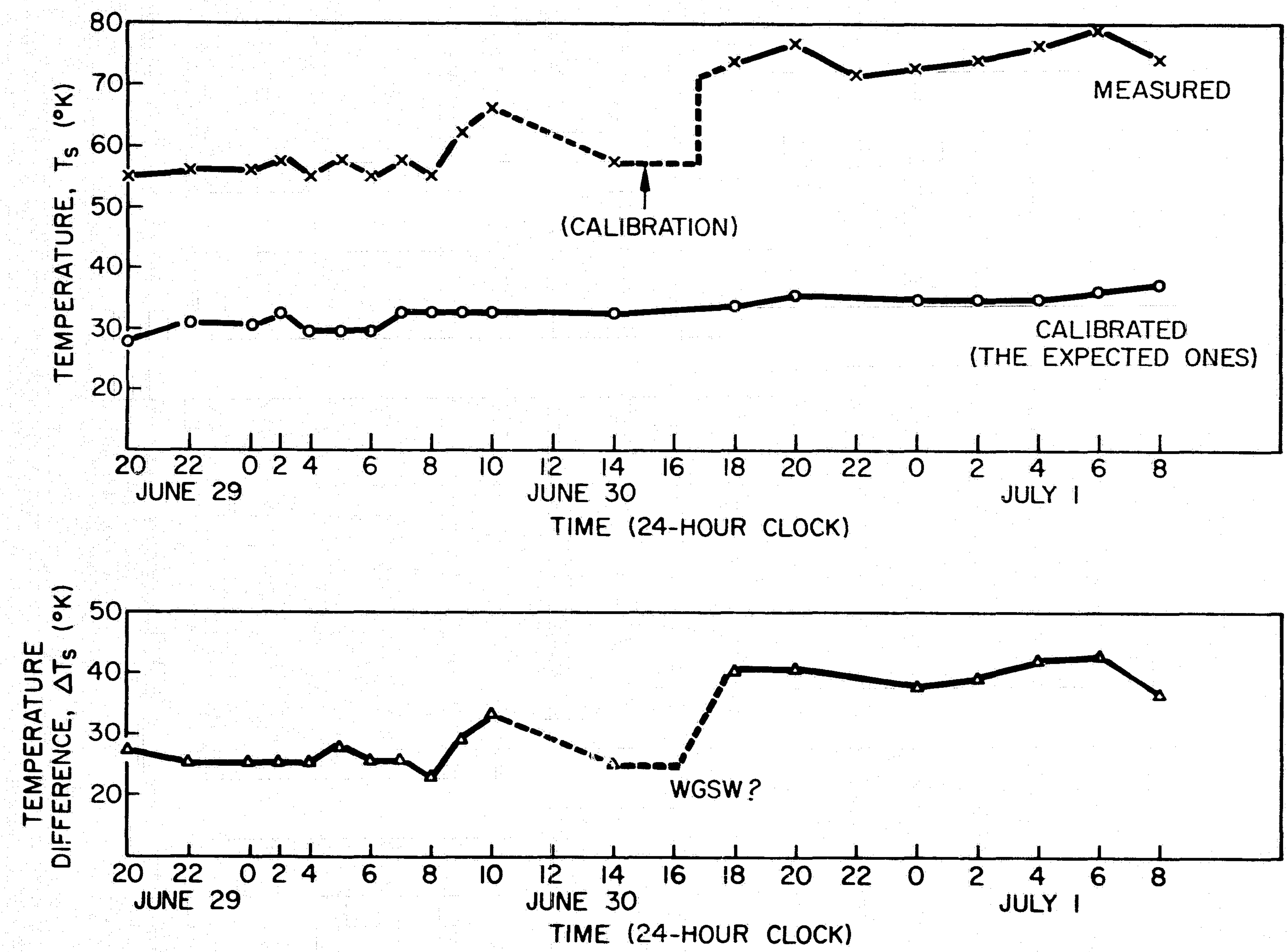

Figure B.3. Two-hourly change for 35 GHz radiometer.

APPENDIX C

Seasonal Sky Temperature Range due to Water Vapor for the Stations Participating in the ATS-V Millimeter Wave Experiment

The 16 GHz and 35 GHz radiometers which were tested at GSFC by the author are to be used at Rosman, North Carolina during the ATS-V Millimeter Wave Experiment. Continuous recordings will be made of the sky temperature along the slant path from the Rosman ground terminal to the ATS-V. An attempt will be made to correlate the radiometric data with propagation data being received from the 15 GHz and 31 GHz beacons on board the spacecraft.

Of equal interest, it is also important to determine if the calculated values of sky temperature variation due to water vapor content agree with the actual values. Consequently as a follow-on endeavor for testing the radiometers, calculations have been carried out, to give the expected sky temperature changes in February and August. The method of calculating the sky temperature change due to the water content is as follows.

1. For the 15 GHz loss and water vapor, (Reference 3)

$$a_1 = 0.055 + 0.004\,\rho;$$

For the 35 GHz loss and water vapor,

$$a_2 = 0.17 + 0.013\,\rho;$$

where a_1, a_2 are the losses in dB and ρ is the water vapor content.

2. The values of absolute humidity expected to be exceeded 99%, 50%, and 1% of the time during February and August can be found in Figures 7.3-7.8 of Reference 2.

3. "Loss" is converted to into α (fractional transmission coefficient).

4. $T_s = (1 - \alpha^{\sec\phi})\,T_m$,

where ϕ is the zenith angle at these stations.

5. $T_m = 270°K$ at 15 GHz.

(There is not a great difference, in sky temperature even if T_m is $\sim$ 280°K.)

6. At 35 GHz,

$$T_m = 270°K \ (0 - 5 \ g/m^3 \text{ water vapor content})$$

$$= 278°K \ (5 - 15 \ g/m^3 \text{ water vapor content})$$

$$= 289°K \ (15 - 20 \ g/m^3 \text{ water vapor content}).$$

Calculation results are listed in Table C1, (a) and (b).

Table C-1
Sky Temperature Change Due to Water Content

(a) For 16 GHz Radiometers

Month	Feb.			Aug.		
Humidity Expected to be Exceeded 99, 50, 1% of the Time	1%	50%	99%	1%	50%	99%
1. Rosman (N.C.) (Brevard)	6	7	9°K	9	11	14°K
2. NELC (Calif.)	6	7	8°K	8	9	11°K
3. U of T (Texas)	5	6	7°K	7	9	10°K
4. OSU (Ohio)	6	7	9°K	8	11	13°K
5. Wash. D.C.	7	8	11°K	11	13	16°K

(b) For 35 GHz Radiometers

Month	Feb.		Aug.	
Humidity Expected to be Exceeded 99 and 1% of the Time	1%	99%	1%	99%
1. Rosman (N.C.) (Brevard)	18	28°K	27	41°K
2. NELC (Calif.)	17	25°K	22	33°K
3. U of T (Texas)	16	24°K	21	33°K
4. OSU (Ohio)	18	28°K	26	40°K
5. Wash. D.C.	20	30°K	31	47°K

APPENDIX D

Correction for the Energy Distribution Pattern for both Radiometer Antennas

The antenna pattern of the 16 GHz radiometer was not obtained until after the analytical portion of this paper was completed. Therefore, a correction must be employed for Section 3.3.

In Figure D.1 are shown the antenna patterns measured in the E plane and the H plane for the 16 GHz radiometer antenna. Scale reduction into half of the 16 GHz holizontal angle values may be applied to the 35 GHz radiometer antenna (parenthetic numbers).

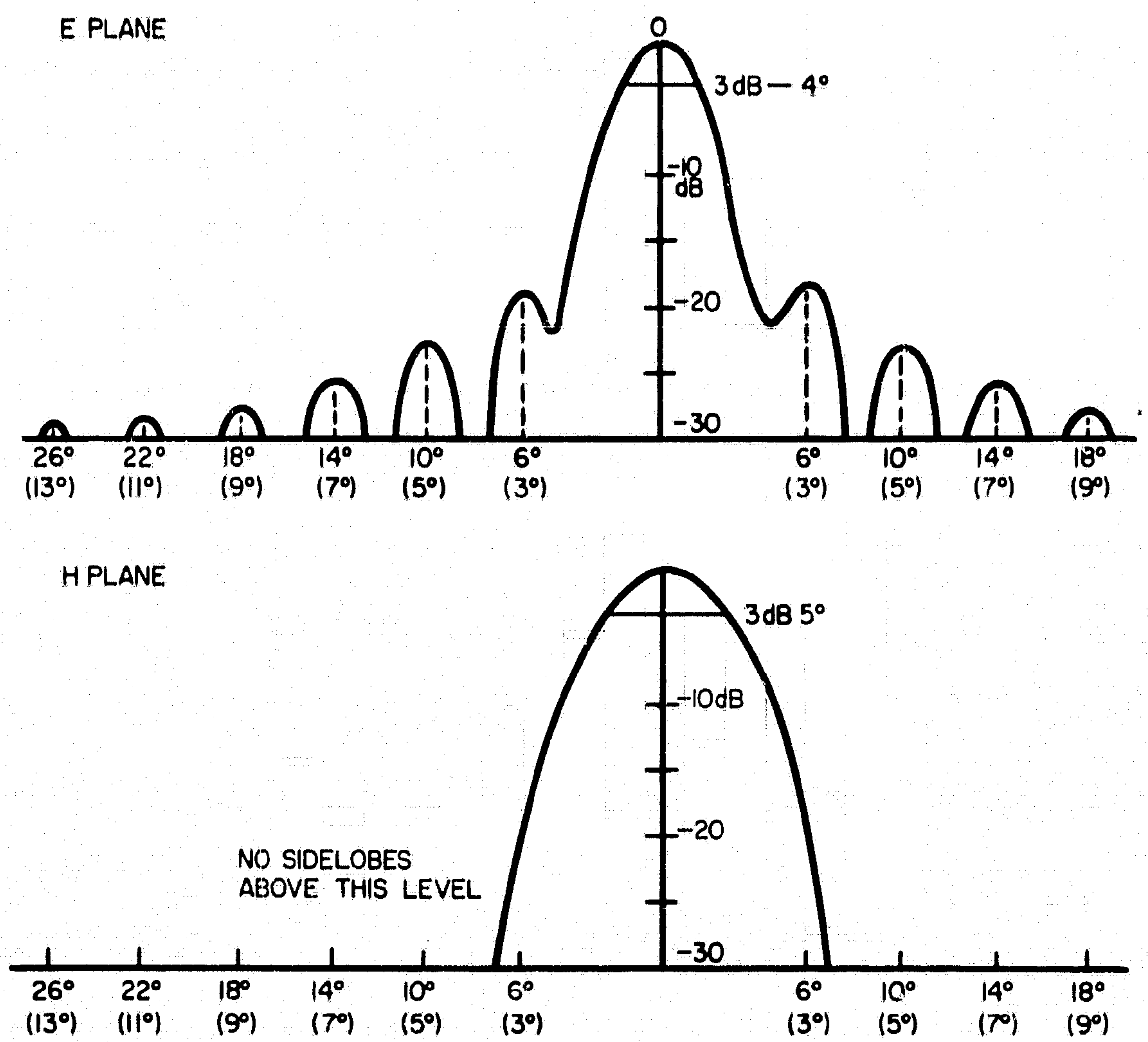

Figure D.1. Actual antenna pattern for 16 GHz 1-foot antenna.

In the H plane pattern, the sidelobes are fairly low under 30 dB and the effective temperature increase due to them is negligible. Therefore, only the E plane pattern need be considered in the investigation of the temperature increase due to sidelobes. By measuring the area of antenna pattern, approximate energy distribution for the 16 GHz radiometer antenna is obtained (Table D.1).

Table D.1

Main beam 0 - ± 5°	66%	For 35 GHz, Angle values are about half of these interpolated from the values of
side lobes - ± 20°	30%	
side lobes ± 60°	3%	
side lobes ±180°	1%	

It can be seen that 99% of all the energy falls within ±60° for the 16 GHz radiometer and within ±30° for the 35 GHz radiometer. The same technique which was used in Section 3.3 can be applied here for the temperature increase due to sidelobes.

Slight changes can be found in the estimates of the temperature increase due to sidelobes intersecting the ground: 2°K for 16 GHz and 1°K for 35 GHz can be obtained for the temperature increase due to ground thermal emission.

Thus, overall, 2.5°K at 16 GHz and 7.5°K at 35 GHz seem to be the values of the temperature increase due to sidelobes at zenith.